Monolithic local subcell DG/FV convex property preserving scheme

François Vilar

Institut Montpelliérain Alexander Grothendieck, Université de Montpellier

JOMA 2023

Scalar conservation law

- $\partial_t u(\mathbf{x},t) + \nabla_x \cdot \mathbf{F}(u(\mathbf{x},t)) = 0, \qquad (\mathbf{x},t) \in \omega \times [0,T]$
- $u(\mathbf{x},0) = u_0(\mathbf{x}), \qquad \mathbf{x} \in \omega$

$(k+1)^{\text{th}}$ order semi-discretization

- $\{\omega_c\}_c$ a partition of ω, such that $\omega = \bigcup_c \omega_c$
- $u_h(\mathbf{x},t)$ the numerical solution, such that $u_{h|\omega_c} = u_h^c \in \mathbb{P}^k(\omega_c)$

$$u_h^c(\mathbf{x},t) = \sum_{m=1}^{N_k} u_m^c(t)\,\sigma_m^c(\mathbf{x})$$

- $\{\sigma_m^c\}_{m=1,\dots,N_k}$ a basis of $\mathbb{P}^k(\omega_c)$, with $N_k = \frac{(k+1)(k+2)}{2}$ in 2D.

Local variational formulation on ω_c

- $\displaystyle\int_{\omega_c} \frac{\partial u_h^c}{\partial t}\,\psi \,\mathrm{d}V = \int_{\omega_c} \mathbf{F}(u_h^c) \cdot \nabla_x \psi \,\mathrm{d}V - \int_{\partial\omega_c} \psi\, \mathcal{F}_n \,\mathrm{d}S, \qquad \forall\, \psi \in \mathbb{P}^k(\omega_c)$
- $\mathcal{F}_n = \mathcal{F}\left(u_h^c, u_h^v, \mathbf{n}\right)$ numerical flux

History

- Introduced by Reed and Hill in 1973 in the frame of the neutron transport
- Major development and improvements by B. Cockburn and C.-W. Shu in a series of seminal papers

Procedure

- Local variational formulation
- Piecewise polynomial approximation of the solution in the cells
- Choice of the numerical fluxes
- Time integration

Advantages

- Natural extension of Finite Volume method
- Excellent analytical properties (L_2 stability, $hp-$adaptivity, ...)
- Extremely high accuracy (superconvergent for scalar conservation laws)
- Compact stencil (involve only face neighboring cells)

Numerical example: solid body rotation

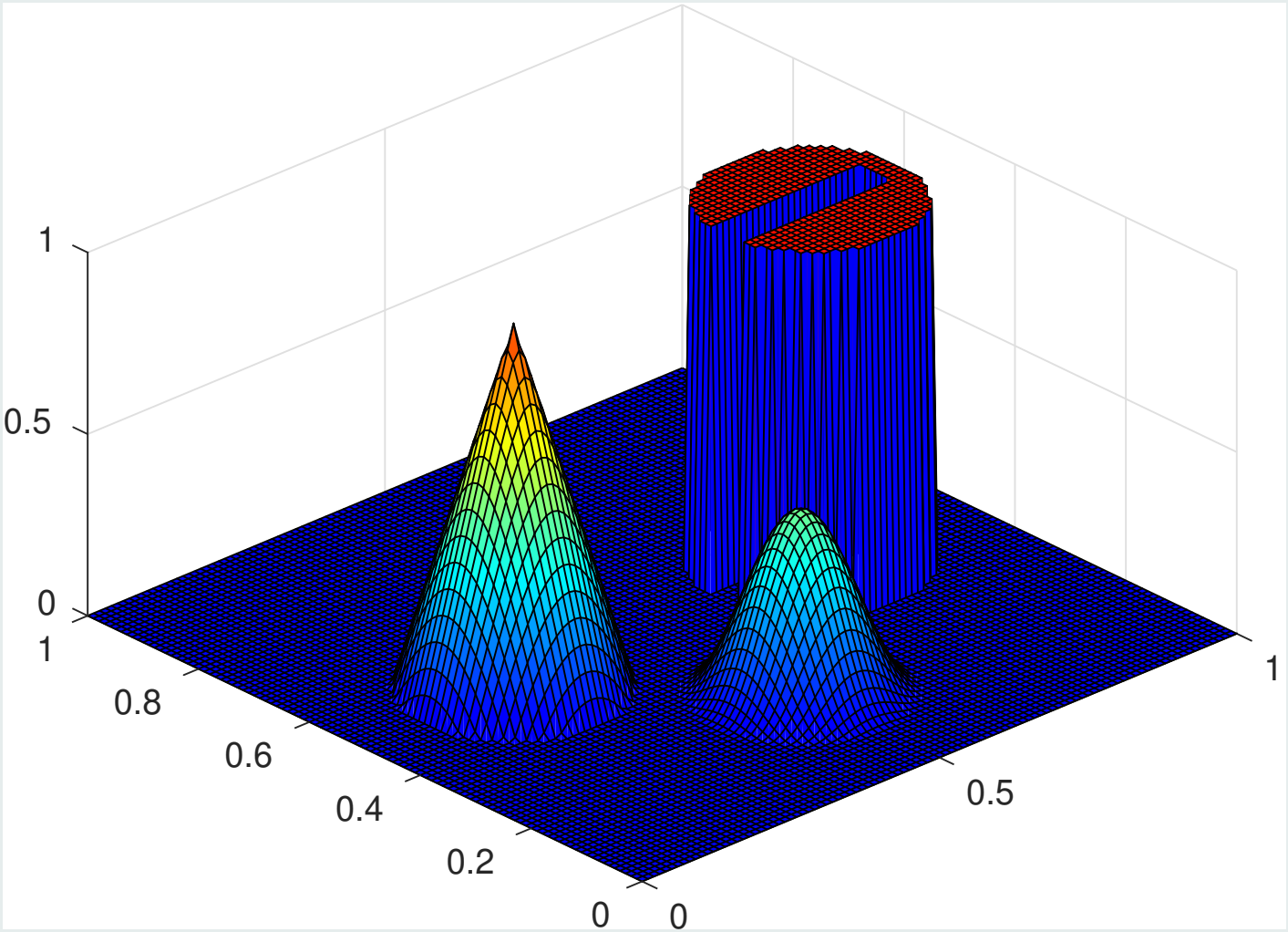

Figure : Rotation of composite signal: initial solution

Roughly constant number of degrees of freedom

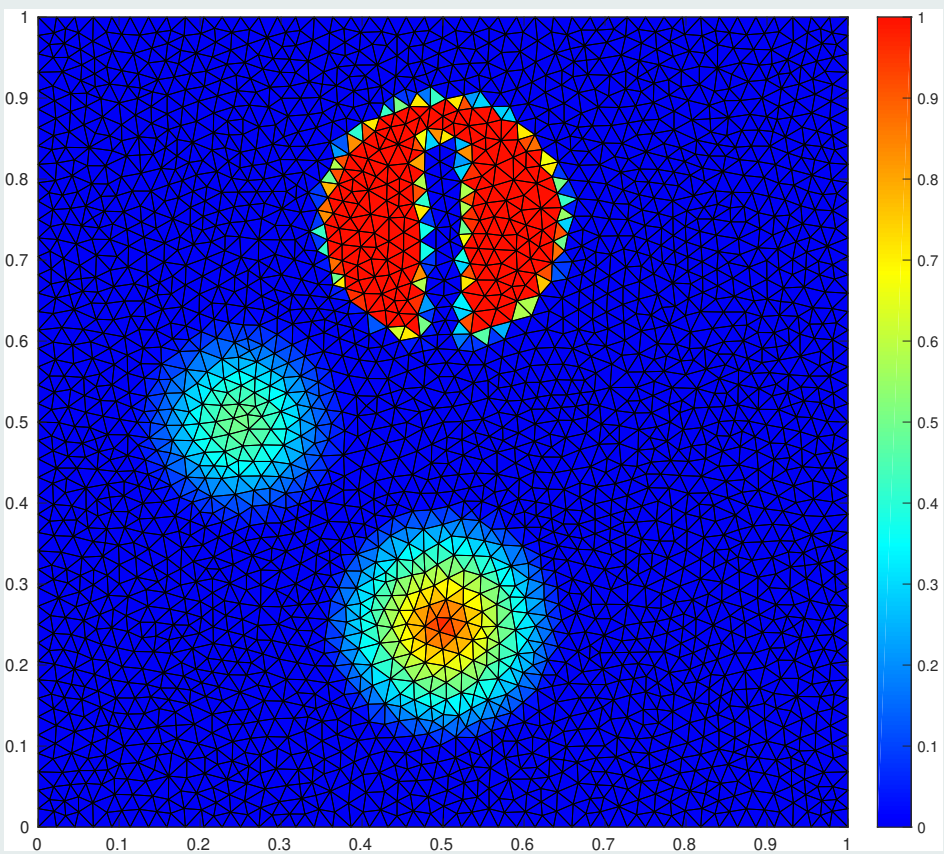

(a) 1st order on 5154 cells

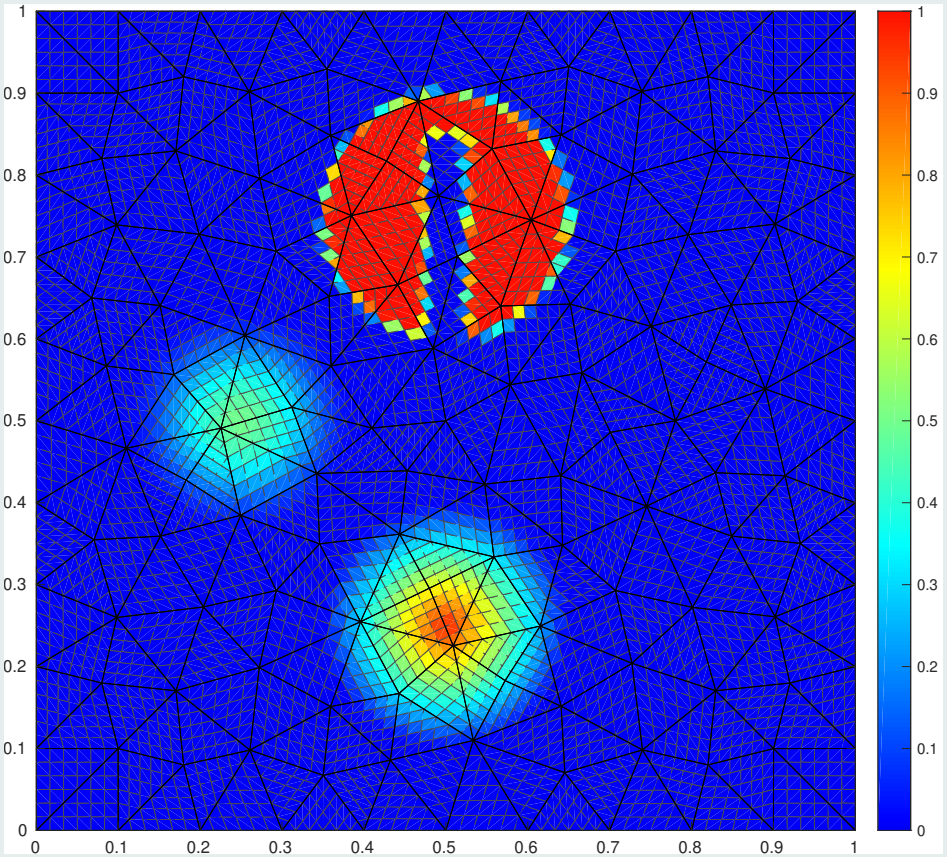

(b) 6th order on 242 cells (5082 DoF)

Figure : Rotation of composite signal: initial solution

Subcell resolution of DG scheme

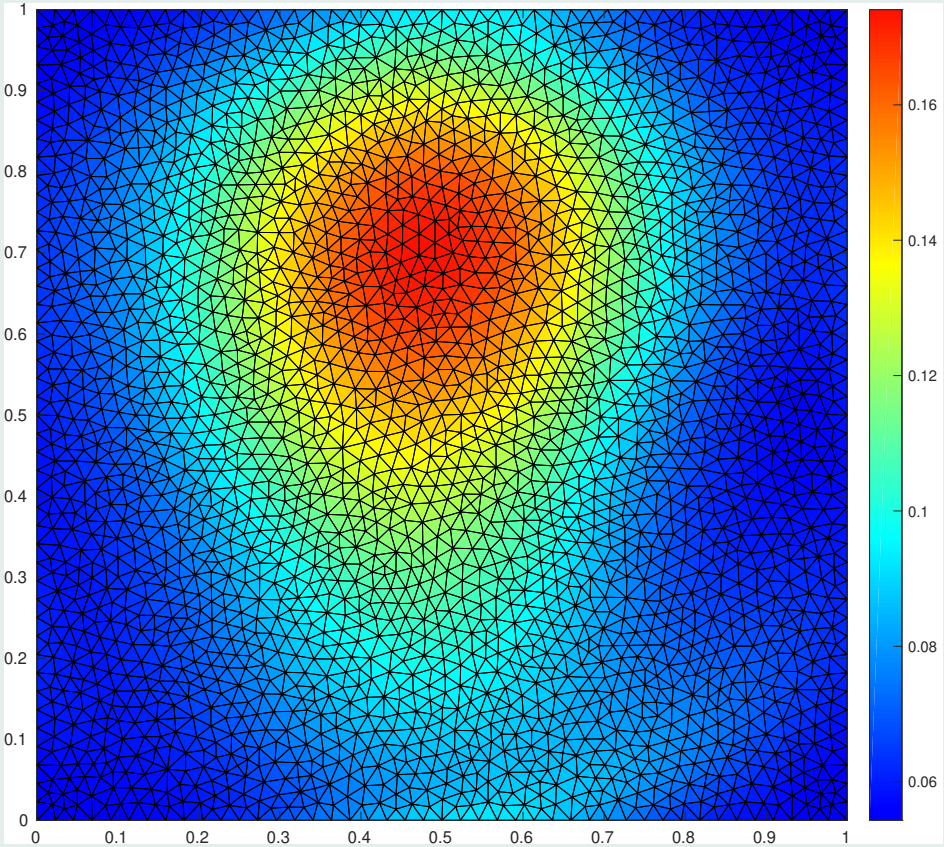

(c) 1st order on 5154 cells

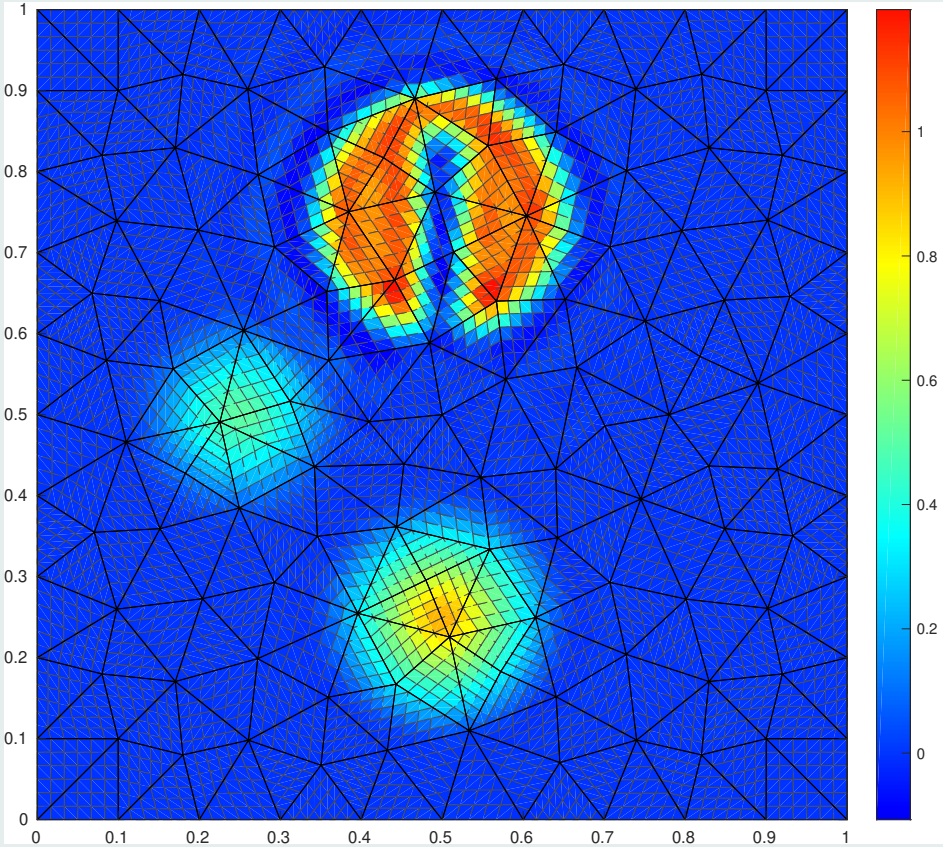

(d) 6th order on 242 cells (5082 DoF)

Figure : Rotation of composite signal after one period: subcells mean value

Subcell resolution of DG scheme

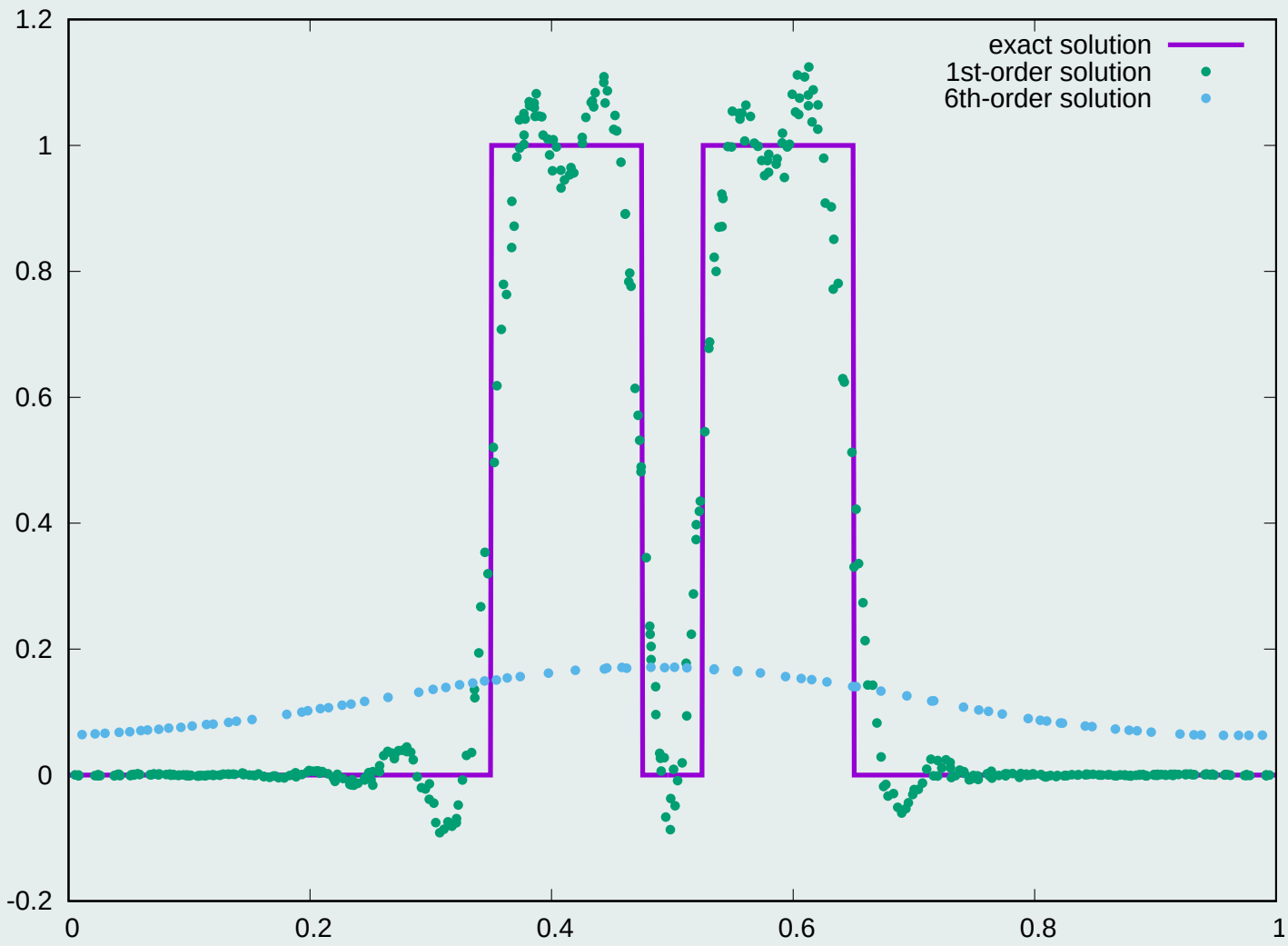

Figure : Rotation of composite signal after one period: profiles for $y = 0.75$

Buckley non-convex flux problem

$$F(u) = \frac{4\,u^2}{4\,u^2+(1-u)^2}$$

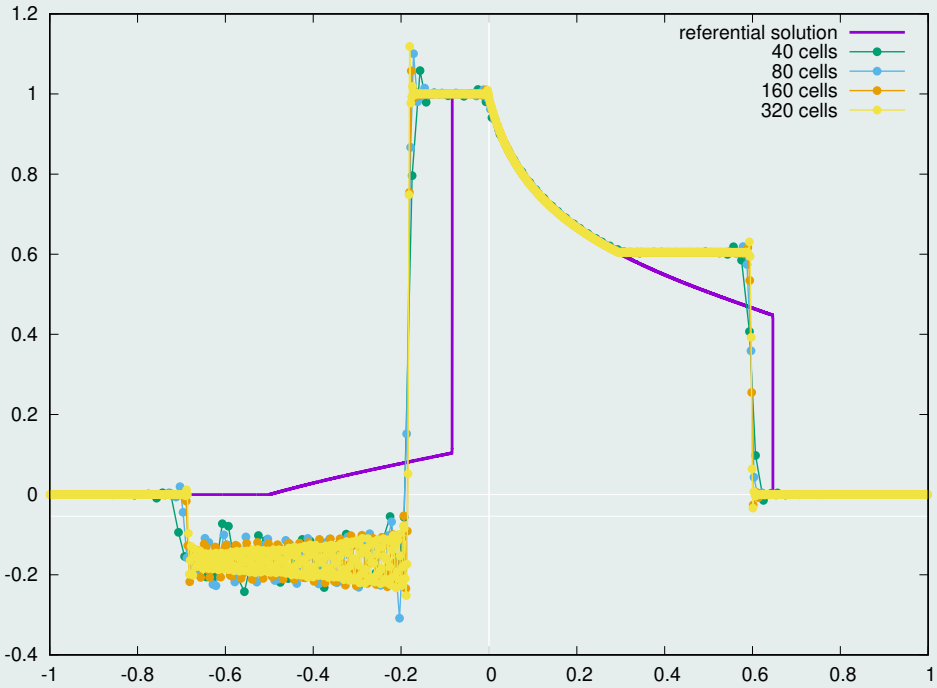

(a) Non-entropic behavior

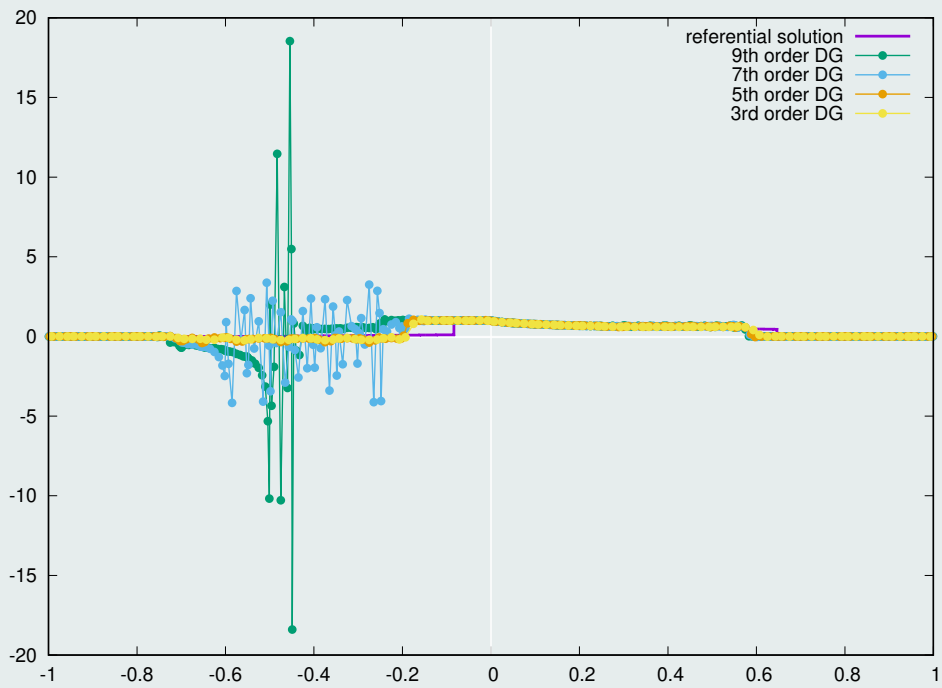

(b) Aliasing phenomenon

Figure : Uncorrected DG solution for the Buckley non-convex flux case where

Gibbs phenomenon and non-admissible solution

- High-order schemes leads to spurious oscillations near discontinuities
- Non-admissible solution potentially leading to a crash
- Vast literature of how prevent this phenomenon to happen:

$$\Longrightarrow \quad \textit{a priori} \text{ and } \textit{a posteriori} \text{ limitations}$$

A priori limitation

- Artificial viscosity
- Flux limitation
- Slope/moment limiter
- Hierarchical limiter
- ENO/WENO limiter

A posteriori limitation

- MOOD (“Multi-dimensional Optimal Order Detection”)
- Subcell finite volume limitation
- **Subcell limitation through flux reconstruction**

Admissible numerical solution

- Maximum principle / positivity preserving
- Ensure a correct entropic behavior

Spurious oscillations

- Discrete maximum principle
- Relaxing condition for smooth extrema

Methodology

Blend, at the subcell scale, high-order DG and 1st-order FV

F. VILAR, *A Posteriori Correction of High-Order DG Scheme through Subcell Finite Volume Formulation and Flux Reconstruction.* JCP, 2018.

F. VILAR AND **R. ABGRALL**, *A posteriori local subcell correction of DG schemes through Finite Volume reformulation on unstructured grids.* SIAM Sci. Comp., 2022. **Under revision.**

DG as a subcell Finite Volume

- Rewrite DG scheme as a FV-like scheme on a subgrid

Cell subdivision into $N_S \geq N_k$ subcells

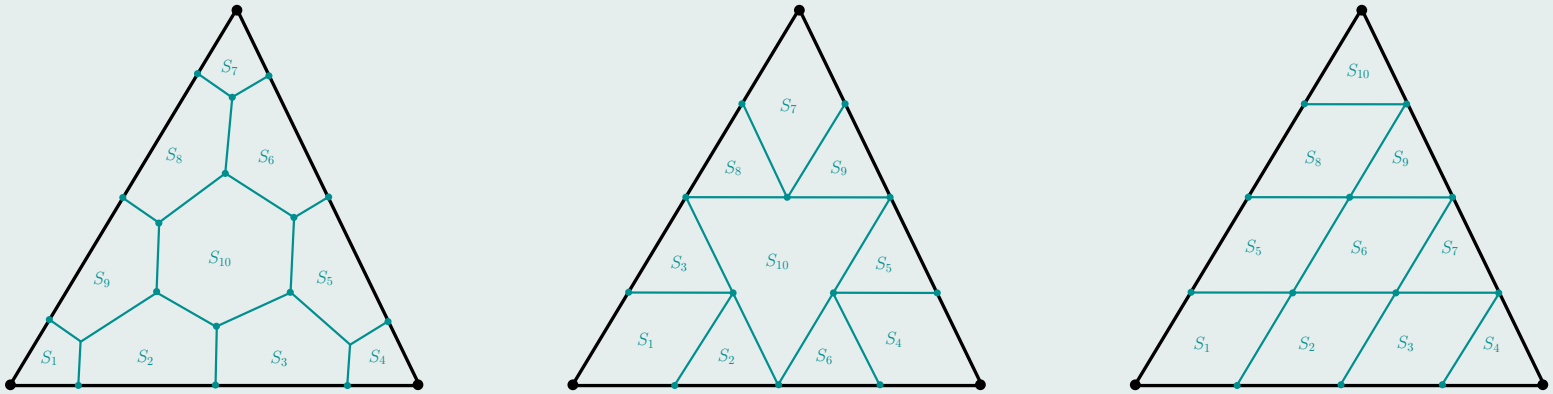

Figure : Examples of $N_s = N_k$ subdivision for $\mathbb{P}^3$ DG scheme on a triangle

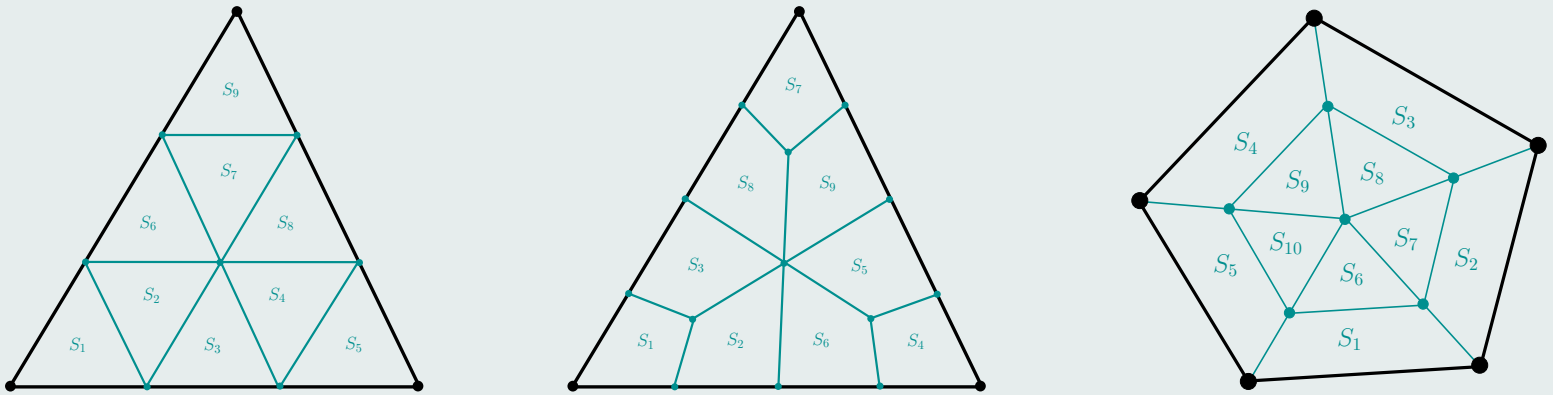

Figure : Examples of $N_S \geq N_k$ subdivision

DG schemes through residuals

- $$\sum_{m=1}^{N_k} \frac{\mathrm{d}\, u_m^c}{\mathrm{d}t} \int_{\omega_c} \sigma_m \sigma_p \,\mathrm{d}V = \int_{\omega_c} \mathbf{F}(u_h^c) \cdot \nabla_x \sigma_p \,\mathrm{d}V - \int_{\partial\omega_c} \sigma_p \,\mathcal{F}_n \,\mathrm{d}S, \quad \forall\, p \in [\![1, N_k]\!]$$

$$\Longrightarrow \qquad \boxed{M_c \frac{\mathrm{d}\, U_c}{\mathrm{d}t} = \Phi_c}$$

- $(U_c)_m = u_m^c$ — Solution moments
- $(M_c)_{mp} = \displaystyle\int_{\omega_c} \sigma_m \sigma_p \,\mathrm{d}V$ — Mass matrix
- $(\Phi_c)_m = \displaystyle\int_{\omega_c} \mathbf{F}(u_h^c) \cdot \nabla_x \sigma_m \,\mathrm{d}V - \int_{\partial\omega_c} \sigma_m \,\mathcal{F}_n \,\mathrm{d}S$ — DG residuals

Subdivision and definition

- ω_c is subdivided into N_s subcells S_m^c
- Let us define $\overline{\psi}_m^c = \dfrac{1}{|S_m^c|} \displaystyle\int_{S_m^c} \psi \,\mathrm{d}V$ the subcell mean value

Submean values

- $\overline{u}_m^c = \dfrac{1}{|S_m^c|} \displaystyle\sum_{q=1}^{N_k} u_q^c \int_{S_m^c} \sigma_q \, \mathrm{d}V \quad \Longrightarrow \quad \boxed{\overline{U}_c = P_c \, U_c}$
- $(\overline{U}_c)_m = \overline{u}_m^c$ Submean values
- $(P_c)_{mp} = \dfrac{1}{|S_m^c|} \displaystyle\int_{S_m^c} \sigma_p \, \mathrm{d}V$ Projection matrix

$$\Longrightarrow \quad \boxed{\frac{\mathrm{d}\,\overline{U}_c}{\mathrm{d}t} = P_c \, M_c^{-1} \, \Phi_c}$$

Admissibility of the cell sub-partition into subcells

- $P_c^{\mathrm{t}} P_c$ **has to be non-singular**

$$\Longrightarrow \quad \boxed{U_c = (P_c^{\mathrm{t}} P_c)^{-1} P_c^{\mathrm{t}} \overline{U}_c}$$ Least square procedure

- If $N_s = N_k$, $\overline{U}_c = P_c \, U_c \iff U_c = P_c^{-1} \overline{U}_c$

Subcell Finite Volume: reconstructed fluxes

- Let us introduce the **reconstructed fluxes** such that

$$\boxed{\frac{\mathrm{d}\,\overline{u}_m^c}{\mathrm{d}t} = -\frac{1}{|S_m^c|}\int_{\partial S_m^c} \widehat{F}_n \,\mathrm{d}S}$$

- Let $\mathcal{V}_m^c$ be the set of face neighboring subcells of S_m^c

$$\frac{\mathrm{d}\,\overline{u}_m^c}{\mathrm{d}t} = -\frac{1}{|S_m^c|}\sum_{S_p^v \in \mathcal{V}_m^c}\int_{f_{mp}^c} \widehat{F}_n \,\mathrm{d}S$$

- We impose that on the boundary of cell ω_c

$$\boxed{\widehat{F}_{n|\partial\omega_c} = \mathcal{F}_n}$$

- Then, if $\widetilde{\mathcal{V}_m^c}$ stands for the set of face neighboring subcells inside ω_c

$$\frac{\mathrm{d}\,\overline{u}_m^c}{\mathrm{d}t} = -\frac{1}{|S_m^c|}\left(\sum_{S_p^c \in \widetilde{\mathcal{V}_m^c}}\int_{f_{mp}^c} \widehat{F}_n \,\mathrm{d}S + \int_{\partial S_m^c \cap \partial\omega_c} \mathcal{F}_n \,\mathrm{d}S\right)$$

Subcell Finite Volume: reconstructed fluxes

- Taking two subcells S_m^c and S_p^v, the orientation face function ε_{mp}^c writes

$$\varepsilon_{mp}^c = \begin{cases} 1 & \text{if face } f_{mp}^c \text{ is direct or if } f_{mp}^c \subset \partial\omega_c, \\ -1 & \text{if face } f_{mp}^c \text{ is indirect,} \\ 0 & \text{if } S_p^v \notin \mathcal{V}_m^c. \end{cases}$$

- $\displaystyle\int_{f_{mp}^c} \widehat{F_n}\,\mathrm{d}S := \widehat{F_{mp}} = -\widehat{F_{pm}}$ face integrated reconstructed flux

$$\boxed{\frac{\mathrm{d}\,\overline{u}_m^c}{\mathrm{d}t} = -\frac{1}{|S_m^c|}\left(\sum_{S_p^c \in \widetilde{\mathcal{V}_m^c}} \widehat{F_{mp}} + \int_{\partial S_m^c \cap \partial\omega_c} \mathcal{F}_n\,\mathrm{d}S\right)}$$

- $(B_c)_m = \displaystyle\int_{\partial S_m^c \cap \partial\omega_c} \mathcal{F}_n\,\mathrm{d}S$ Cell boundary contribution
- $(A_c)_{mp} = \varepsilon_{mp}^c$ Adjacency matrix
- $D_c = \mathrm{diag}\left(|S_1^c|, \ldots, |S_{N_k}^c|\right)$ Subcells volume matrix

Subcell Finite Volume: reconstructed fluxes

- Let $\widehat{F_c}$ be the vector containing all the interior faces reconstructed fluxes
- The subcell mean values governing equations yield the following system

$$-A_c\,\widehat{F_c} = D_c\,\frac{\mathrm{d}\,\overline{U}_c}{\mathrm{d}t} + B_c$$

Graph Laplacian technique

- $A_c \in \mathcal{M}_{N_s \times N_f^c}$ with N_f^c the number of interior faces
- $A_c^{\mathrm{t}}\,\mathbf{1} = \mathbf{0}$ where $\mathbf{1} = (1,\ldots,1)^{\mathrm{t}} \in \mathbb{R}^{N_s}$

R. ABGRALL, *Some Remarks about Conservation for Residual Distribution Schemes.* Methods Appl. Math., 18:327-351, 2018.

- Let $\mathcal{L}_c^{-1}$ be the inverse of $L_c = A_c\,A_c^{\mathrm{t}}$ on the orthogonal of its kernel

$$\mathcal{L}_c^{-1} = (L_c + \lambda\,\Pi)^{-1} - \frac{1}{\lambda}\,\Pi \qquad \forall \lambda \neq 0$$

- $\Pi = \frac{1}{N_s}\,(\mathbf{1} \otimes \mathbf{1}) \in \mathcal{M}_{N_s}$

Graph Laplacian technique

- Finally, we obtain the following definition of the reconstructed fluxes

$$\boxed{\widehat{F_c} = -A_c^{\mathrm{t}}\,\mathcal{L}_c^{-1}\left(D_c\,P_c\,M_c^{-1}\,\Phi_c + B_c\right)}$$

remark

- The only terms depending on the time are Φ_c and B_c

One-dimensional case: $N_f^i = N_s - 1$

- $A_i = \begin{pmatrix} 1 & 0 & \dots & 0 \\ -1 & 1 & \ddots & \vdots \\ 0 & \ddots & \ddots & \vdots \\ \vdots & \ddots & \ddots & 1 \\ 0 & \dots & \dots & -1 \end{pmatrix}$, $L_i = A_i\,A_i^{\mathrm{t}} = \begin{pmatrix} 1 & -1 & 0 & \dots & 0 \\ -1 & 2 & 1 & \ddots & \vdots \\ 0 & \ddots & \ddots & \ddots & \vdots \\ \vdots & \dots & -1 & 2 & 1 \\ 0 & \dots & 0 & -1 & 1 \end{pmatrix}$
- $B_i = \left(-\mathcal{F}_{i-\frac{1}{2}}, 0, \dots, 0, \mathcal{F}_{i+\frac{1}{2}}\right)^{\mathrm{t}}$

Different cell subdivisions $\mathbb{P}^3$

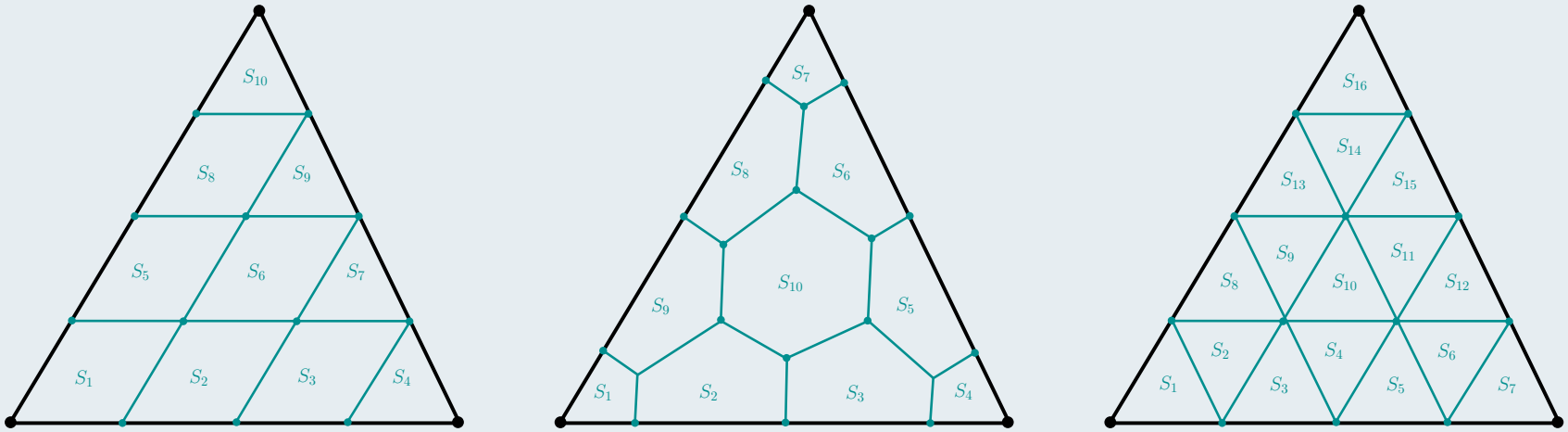

Figure : Examples of easily generalizable subdivisions for a triangle cell

DG is DG

- **Only the functional space matters**
- **The cell subdivision has no influence on the resulting scheme**
- **Even in the case where** $N_s > N_k$

Rotation of a composite signal after one full rotation

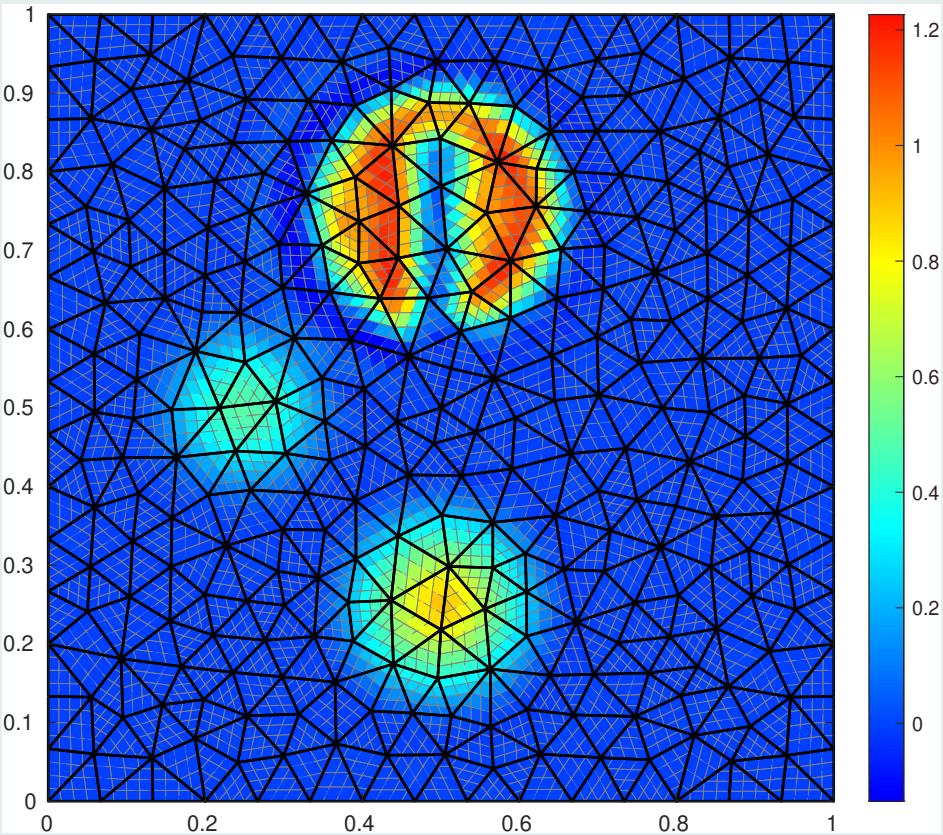

(a) Cartesian subdivision

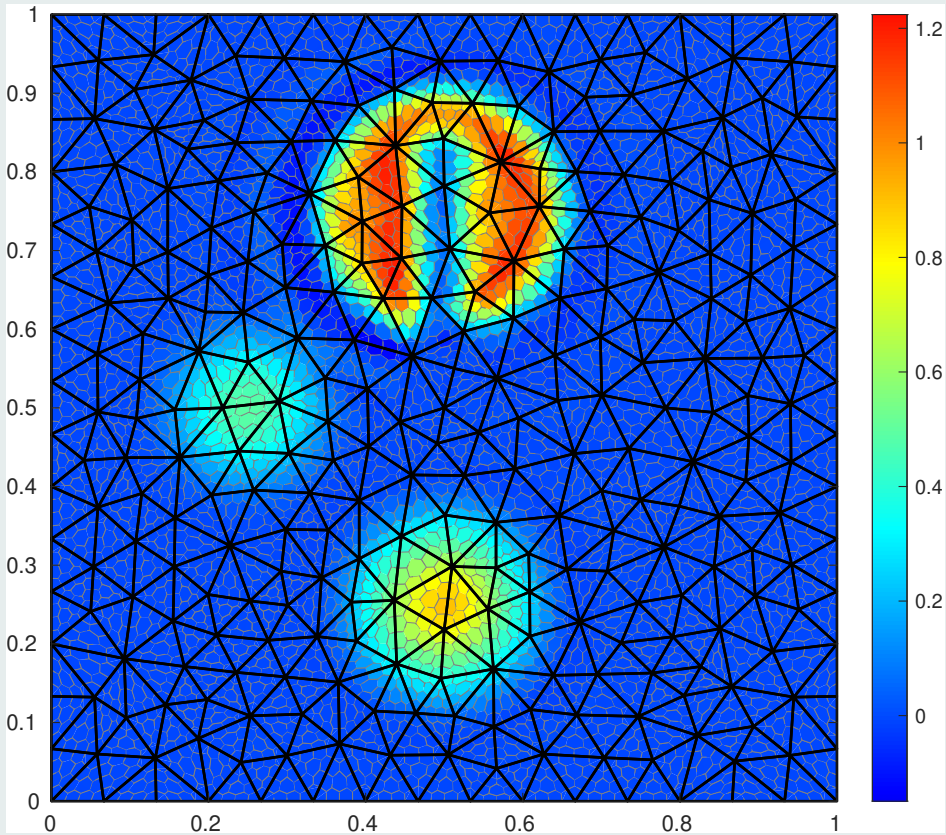

(b) Polygonal subdivision

Figure : $\mathbb{P}^3$ reconstruted flux FV schemes on 576 cells: subcells mean values

Rotation of a composite signal after one full rotation

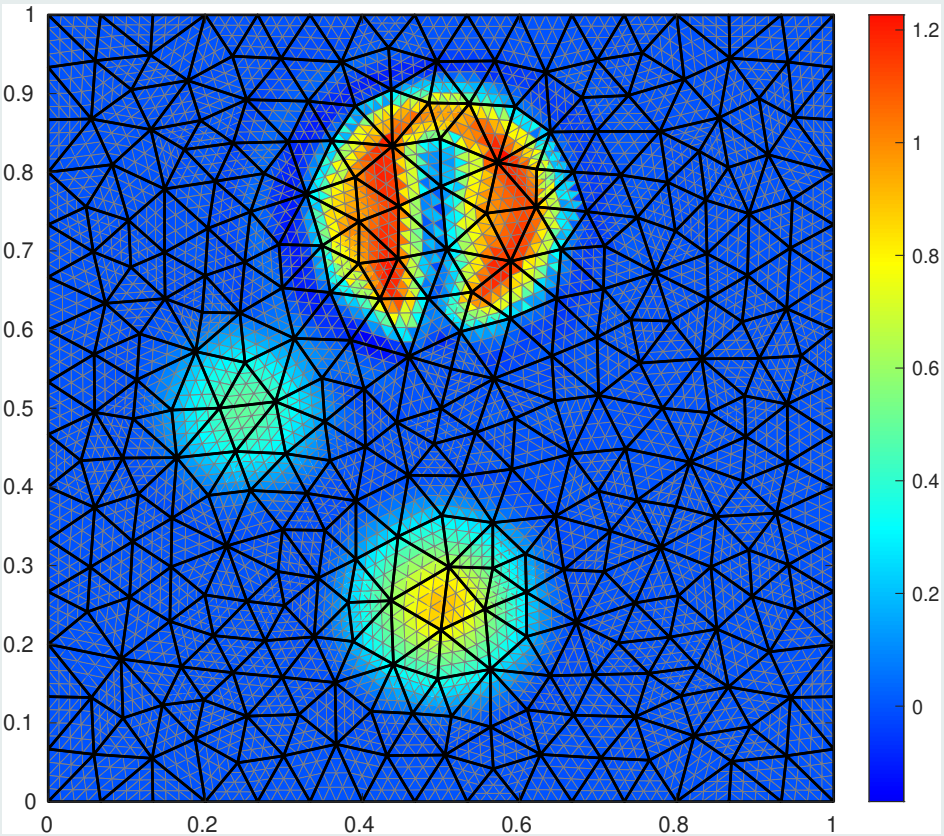

(a) Triangular subdivision

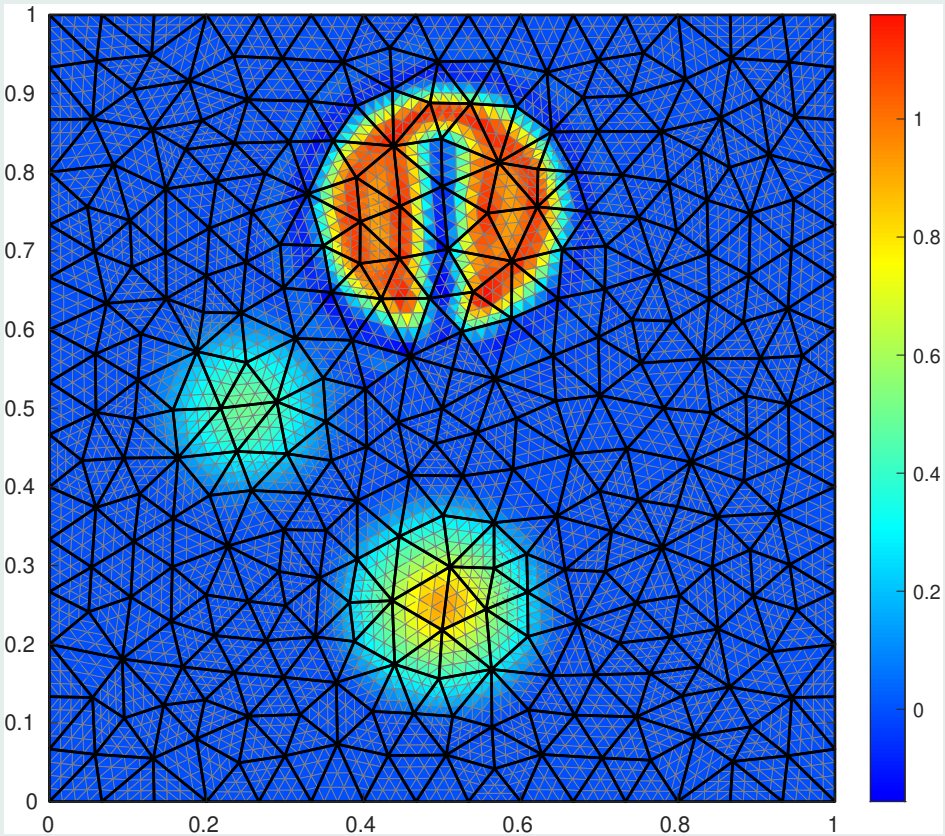

(b) Enriched-DG triangular subdivision

Figure : $\mathbb{P}^3$ and $\mathbb{P}^{4+\frac{1}{6}}$ reconstruted flux FV schemes on 576 cells: subcells mean values

Rotation of a composite signal after one full rotation

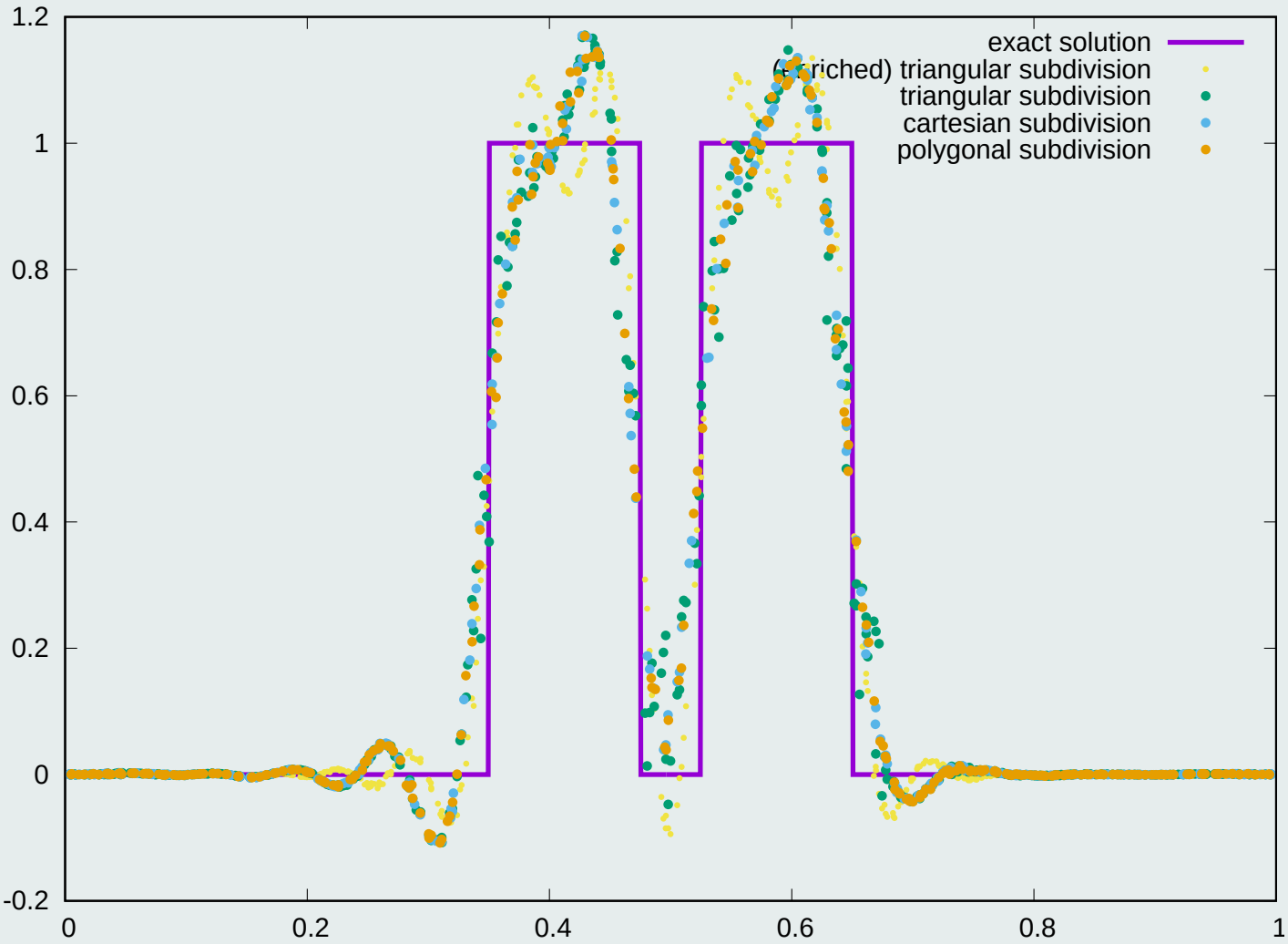

Figure : Reconstruted flux FV schemes on 576 cells: solution profiles for $y = 0.75$

Definitions

$\overline{u}^i_0 := \overline{u}^{i-1}_{N_s}$ and $\overline{u}^i_{N_s+1} := \overline{u}^{i+1}_1$

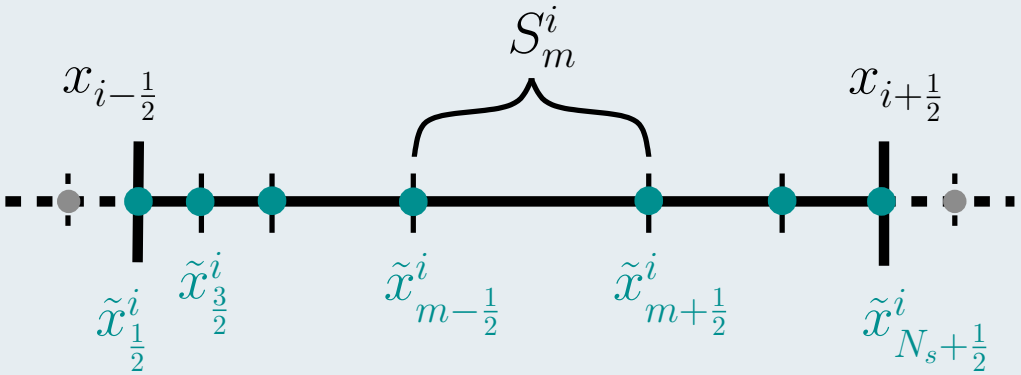

- $\widehat{F^i_{m+\frac{1}{2}}}$ high-order reconstructed flux

- $\mathcal{F}^i_{m+\frac{1}{2}} := \mathcal{F}\left(\overline{u}^i_m, \overline{u}^i_{m+1}\right)$ first-order subcell numerical flux

$$= \frac{F(\overline{u}^i_m) + F(\overline{u}^i_{m+1})}{2} - \frac{\gamma_{m+\frac{1}{2}}}{2}\left(\overline{u}^i_{m+1} - \overline{u}^i_m\right)$$ **E-flux**

- $\widetilde{F^i_{m+\frac{1}{2}}} := \mathcal{F}^i_{m+\frac{1}{2}} + \theta^i_{m+\frac{1}{2}} \underbrace{\left(\widehat{F^i_{m+\frac{1}{2}}} - \mathcal{F}^i_{m+\frac{1}{2}}\right)}_{\Delta F^i_{m+\frac{1}{2}}}$ convex blended flux

Remarks

- We drop superscript ^{i}, as the cell structure is only seen in the construction of the reconstructed fluxes $\widehat{F^{i}_{m+\frac{1}{2}}}$
- We focus on forward Euler (FE) time stepping, as SSP Runge-Kutta can be formulated as convex combinations of FE
- We drop superscript ^{n} when not explicitly needed

Reformulation of the monolithic subcell scheme

- $$\overline{u}_m^{n+1} = \overline{u}_m - \frac{\Delta t}{|S_m|}\left(\widetilde{F_{m+\frac{1}{2}}} - \widetilde{F_{m-\frac{1}{2}}}\right) \pm F(\overline{u}_m) \pm \frac{\Delta t}{|S_m|}\left(\gamma_{m+\frac{1}{2}} + \gamma_{m-\frac{1}{2}}\right)\overline{u}_m$$

$$= \left(1 - \frac{\Delta t}{|S_m|}\left(\gamma_{m+\frac{1}{2}} + \gamma_{m-\frac{1}{2}}\right)\right)\overline{u}_m$$

$$+ \frac{\Delta t}{|S_m|}\gamma_{m+\frac{1}{2}} \underbrace{\left(\overline{u}_m - \frac{\widetilde{F_{m+\frac{1}{2}}} - F(\overline{u}_m)}{\gamma_{m+\frac{1}{2}}}\right)}_{\widetilde{u_{m+\frac{1}{2}}}^{-}} + \frac{\Delta t}{|S_m|}\gamma_{m-\frac{1}{2}} \underbrace{\left(\overline{u}_m + \frac{\widetilde{F_{m-\frac{1}{2}}} - F(\overline{u}_m)}{\gamma_{m-\frac{1}{2}}}\right)}_{\widetilde{u_{m-\frac{1}{2}}}^{+}}$$

Convex combination

- $\lambda_{m\pm\frac{1}{2}} = \dfrac{\Delta t}{|S_m|}\,\gamma_{m\pm\frac{1}{2}}$

$$\boxed{\overline{u}_m^{n+1} = \left(1 - \left(\lambda_{m-\frac{1}{2}} + \lambda_{m+\frac{1}{2}}\right)\right)\overline{u}_m \;+\; \lambda_{m+\frac{1}{2}}\,\widetilde{u_{m+\frac{1}{2}}}^{\,-} \;+\; \lambda_{m-\frac{1}{2}}\,\widetilde{u_{m-\frac{1}{2}}}^{\,+}}$$

- $\Delta t \leq \dfrac{|S_m|}{\gamma_{m-\frac{1}{2}} + \gamma_{m+\frac{1}{2}}}$ CFL condition

Modified Riemann intermediate states

- $$\widetilde{u_{m+\frac{1}{2}}}^{\,-} = \overline{u}_m - \frac{\widetilde{F_{m+\frac{1}{2}}} - F(\overline{u}_m)}{\gamma_{m+\frac{1}{2}}} = \overline{u}_m - \frac{\mathcal{F}_{m+\frac{1}{2}} - F(\overline{u}_m)}{\gamma_{m+\frac{1}{2}}} - \theta_{m+\frac{1}{2}}\frac{\Delta F_{m+\frac{1}{2}}}{\gamma_{m+\frac{1}{2}}}$$

$$= \underbrace{\frac{\overline{u}_m + \overline{u}_{m+1}}{2} - \frac{F(\overline{u}_{m+1}) - F(\overline{u}_m)}{2\,\gamma_{m+\frac{1}{2}}}}_{u^*_{m+\frac{1}{2}}} - \theta_{m+\frac{1}{2}}\frac{\Delta F_{m+\frac{1}{2}}}{\gamma_{m+\frac{1}{2}}}$$

Modified Riemann intermediate states

- $\widetilde{u_{m+\frac{1}{2}}}^{\pm} = u^*_{m+\frac{1}{2}} \pm \theta_{m+\frac{1}{2}} \dfrac{\Delta F_{m+\frac{1}{2}}}{\gamma_{m+\frac{1}{2}}} \quad \Longrightarrow \quad u^*_{m+\frac{1}{2}} = \dfrac{1}{2}\left(\widetilde{u_{m+\frac{1}{2}}}^{-} + \widetilde{u_{m+\frac{1}{2}}}^{+}\right)$

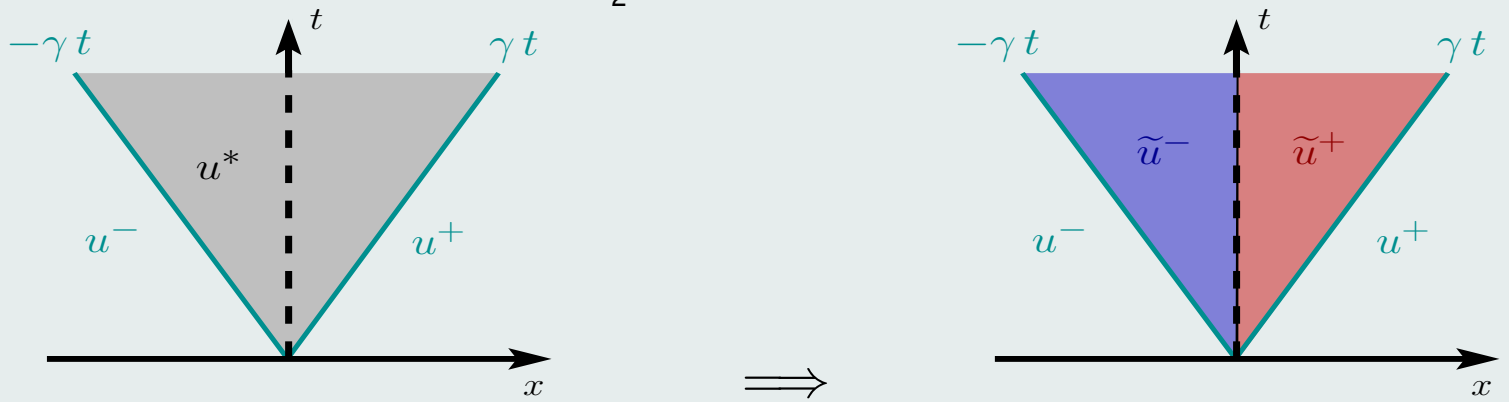

(a) 1st-order situation (b) Blended flux situation

Weak entropic solution average

- $u^* := \dfrac{u^- + u^+}{2} - \dfrac{F(u^+) - F(u^-)}{2\,\gamma}$

$$= \frac{1}{2\,\gamma\,\Delta t} \int_{-\gamma\,\Delta t}^{\gamma\,\Delta t} \mathcal{W}\left(\frac{x}{\Delta t};\, u^-,\, u^+\right) \mathrm{d}x$$

- $\gamma \geq \max\limits_{u \in \mathrm{I}(u^-, u^+)} |F'(u)|$

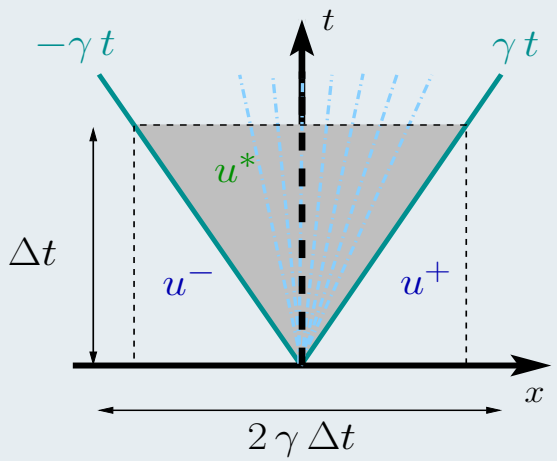

Global maximum principle $\overline{u}_m^{n+1} \in [\alpha, \beta]$

$$\theta_{m+\frac{1}{2}} \leq \min\left(1, \underbrace{\left|\frac{\gamma_{m+\frac{1}{2}}}{\Delta F_{m+\frac{1}{2}}}\right|}_{D_{m+\frac{1}{2}}} \min\left(\beta - u^*_{m+\frac{1}{2}},\, u^*_{m+\frac{1}{2}} - \alpha\right)\right)$$

Local maximum principle $\overline{u}_m^{n+1} \in \mathrm{I}\left(\overline{u}_{m-1}^n, \overline{u}_m^n, \overline{u}_{m+1}^n\right)$

- $\widetilde{u_{m+\frac{1}{2}}}^- \in [\alpha_m, \beta_m] := \mathrm{I}\left(\overline{u}_{m-1}^n, \overline{u}_m^n, \overline{u}_{m+1}^n\right)$
- $\widetilde{u_{m+\frac{1}{2}}}^+ \in [\alpha_{m+1}, \beta_{m+1}] := \mathrm{I}\left(\overline{u}_m^n, \overline{u}_{m+1}^n, \overline{u}_{m+2}^n\right)$

$$\theta_{m+\frac{1}{2}} \leq \min\left(1, |D_{m+\frac{1}{2}}| \begin{cases} \min\left(\beta_{m+1} - u^*_{m+\frac{1}{2}},\, u^*_{m+\frac{1}{2}} - \alpha_m\right) & \text{if } \Delta F_{m+\frac{1}{2}} > 0 \\ \min\left(\beta_m - u^*_{m+\frac{1}{2}},\, u^*_{m+\frac{1}{2}} - \alpha_{m+1}\right) & \text{if } \Delta F_{m+\frac{1}{2}} < 0 \end{cases}\right)$$

- Smooth extrema relaxation to preserve accuracy

Linear advection of a composite signal

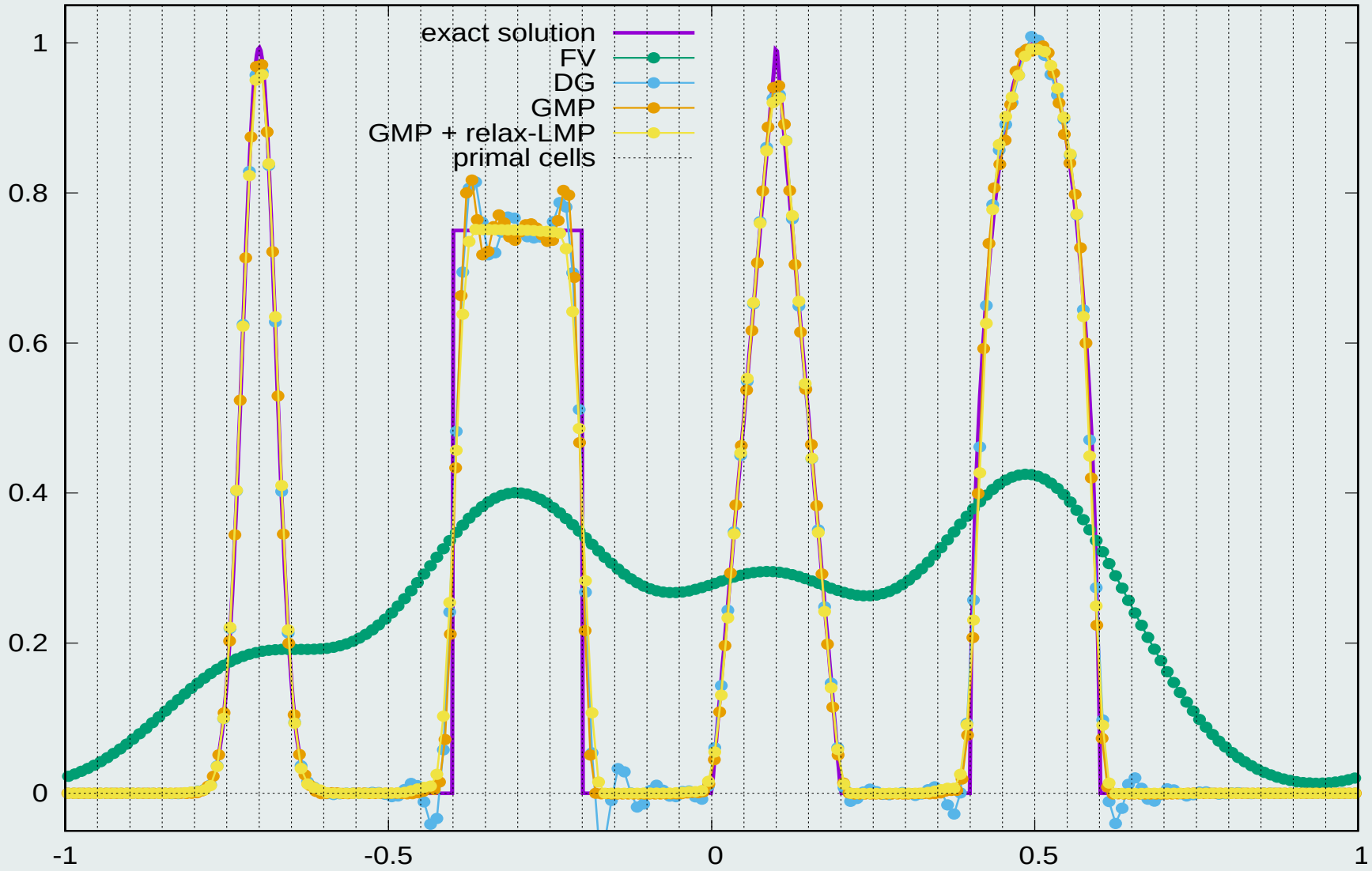

Figure : $\mathbb{P}^5$-DG/FV solutions on 40 cells: submean values

Linear advection of a composite signal

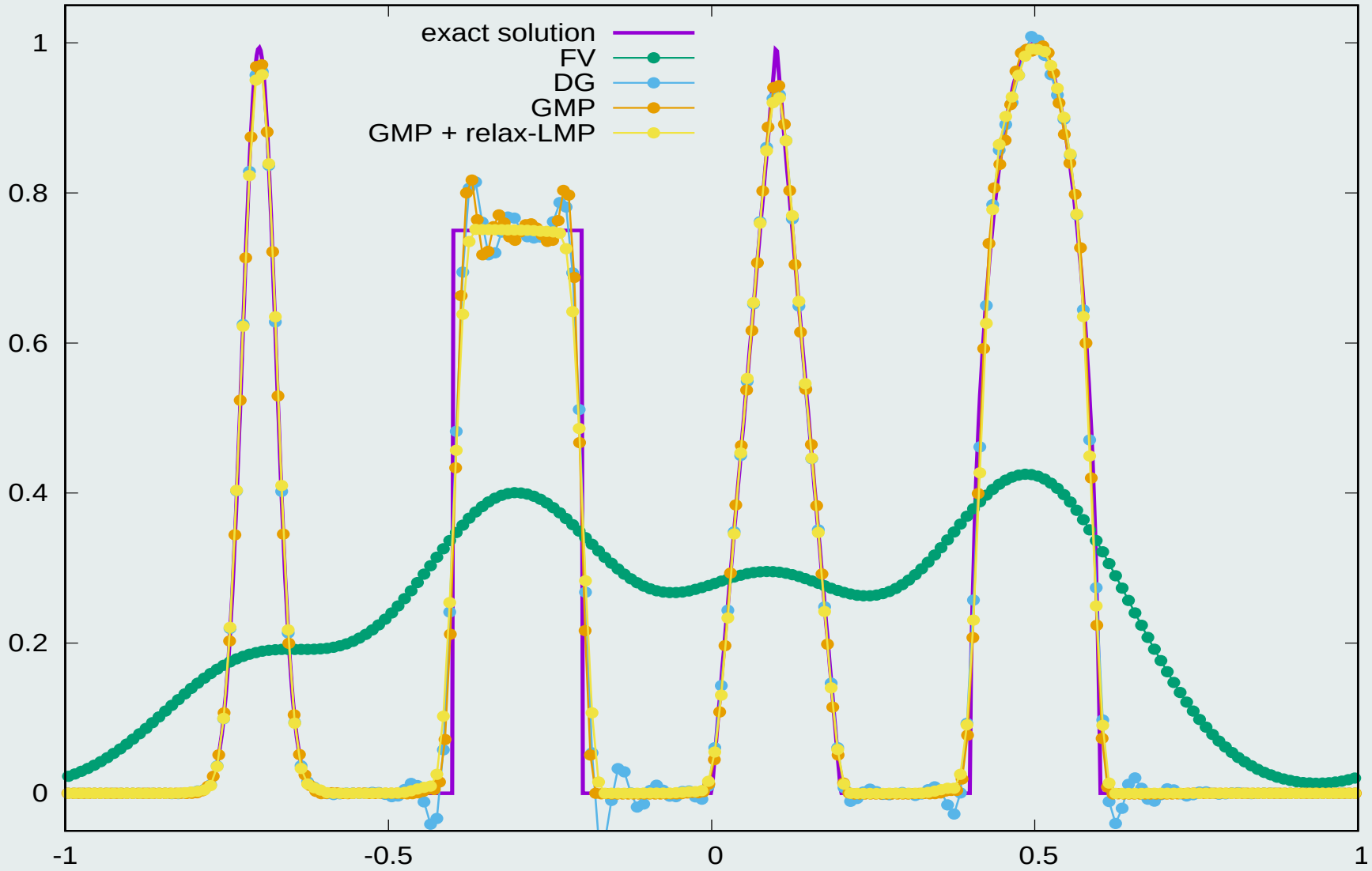

Figure : $\mathbb{P}^5$-DG/FV solutions on 40 cells: submean values

Non-linear non-convex flux Buckley case

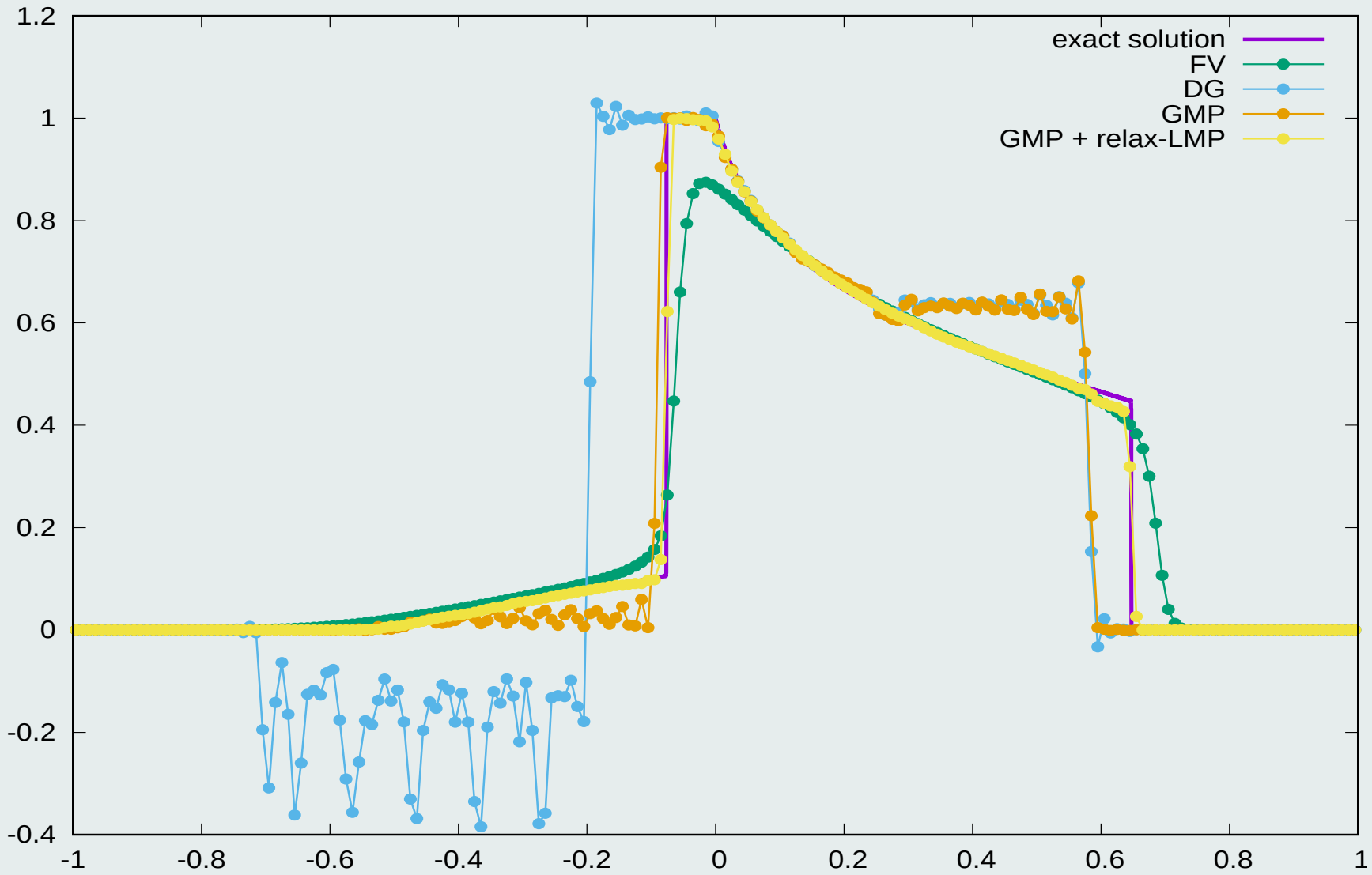

Figure : $\mathbb{P}^4$-DG/FV solutions on 40 cells: submean values

Definitions

- (η, ϕ) entropy - entropy flux
- $v(u) = \eta'(u)$ entropy variable
- $\psi(u) = v(u)\, F(u) - \phi(u)$ entropy potantial
- $\phi^*(u^-, u^+) = \dfrac{\phi(u^-) + \phi(u^+)}{2} - \dfrac{\gamma}{2}\left(\eta(u^+) - \eta(u^-)\right)$
- $\eta(u^*) \leq \eta^* := \dfrac{\eta(u^-) + \eta(u^+)}{2} - \dfrac{\eta(u^+) - \eta(u^-)}{2\,\gamma}$

Subcell entropy stability at the discrete level for all (η, ϕ)

- if $\Delta F_{m+\frac{1}{2}} \,.\, (\overline{u}_{m+1} - \overline{u}_m) > 0$,

$$\theta_{m+\frac{1}{2}} \leq \min\left(1,\ \frac{\left(\gamma_{m+\frac{1}{2}} - \gamma_{\text{God}}\right)\left(\overline{u}_{m+1} - \overline{u}_m\right)}{2\,\Delta F_{m+\frac{1}{2}}}\right)$$

- γ_{God} Godunov viscosity coefficient

Subcell entropy stability at the discrete level for a given (η, ϕ)

- if $\Delta F_{m+\frac{1}{2}} \cdot v\left(u^*_{m+\frac{1}{2}} + \frac{1}{D_{m+\frac{1}{2}}}\right) > 0,$

$$\theta_{m+\frac{1}{2}} \leq \min\left(1, \frac{\left(\eta^*_{m+\frac{1}{2}} - \eta\left(u^*_{m+\frac{1}{2}}\right)\right)\left|D_{m+\frac{1}{2}}\right|}{\left|v\left(u^*_{m+\frac{1}{2}} + \frac{1}{D_{m+\frac{1}{2}}}\right)\right|}\right)$$

- if $\Delta F_{m+\frac{1}{2}} \cdot v\left(u^*_{m+\frac{1}{2}} - \frac{1}{D_{m+\frac{1}{2}}}\right) < 0,$

$$\theta_{m+\frac{1}{2}} \leq \min\left(1, \frac{\left(\eta^*_{m+\frac{1}{2}} - \eta\left(u^*_{m+\frac{1}{2}}\right)\right)\left|D_{m+\frac{1}{2}}\right|}{\left|v\left(u^*_{m+\frac{1}{2}} - \frac{1}{D_{m+\frac{1}{2}}}\right)\right|}\right)$$

Subcell entropy conservation/dissipation at the semi-discrete level for a given (η, ϕ)

- if $\Delta F_{m+\frac{1}{2}} \cdot \left(v\left(\overline{u}_{m+1}\right) - v\left(\overline{u}_{m}\right)\right) > 0$,

$$\theta_{m+\frac{1}{2}} \leq \min\left(1, \frac{\dfrac{\psi\left(\overline{u}_{m+1}\right) - \psi\left(\overline{u}_{m}\right)}{v\left(\overline{u}_{m+1}\right) - \left(\overline{u}_{m}\right)} - \mathcal{F}_{m+\frac{1}{2}}}{\Delta F_{m+\frac{1}{2}}}\right)$$

D. KUZMIN AND **M. QUEZADA DE LUNA**, *Algebraic entropy fixes and convex limiting for continuous finite element discretizations of scalar hyperbolic conservation laws.* Comp. Math. Appl. Mech. Eng., 2020.

A. RUEDA-RAMÍREZ, **B. BOLM**, **D. KUZMIN** AND **G. GASSNER**, *Monolithic Convex Limiting for Legendre-Gauss-Lobatto Discontinuous Galerkin Spectral Element Methods.* Arxiv, 2023.

Cell entropy conservation/dissipation at the semi-discrete level for a given (η, ϕ)

- if $\Delta F_{m+\frac{1}{2}} \cdot \left(\underline{v}_{m+1} - \underline{v}_m\right) > 0$,

$$\theta_{m+\frac{1}{2}} \leq \min\left(1, \frac{\dfrac{\psi\left(u\left(\underline{v}_{m+1}\right)\right) - \psi\left(u\left(\underline{v}_m\right)\right)}{\underline{v}_{m+1} - \underline{v}_m} - \mathcal{F}_{m+\frac{1}{2}}}{\Delta F_{m+\frac{1}{2}}}\right)$$

- $\mathcal{F}_{m+\frac{1}{2}} := \mathcal{F}\left(u\left(\underline{v}_{m+1}\right), u\left(\underline{v}_m\right)\right)$ modified FV numerical flux
- $v_h^i = \sum_{\ell=1}^{k+1} \underline{v}_m^i \, \varphi_m^i \in \mathbb{P}^k$ L^2 projection of $v\left(u_h^i\right)$ onto $\mathbb{P}^k$
- $\left\{\varphi_m^i\right\}_{m=1,\ldots,k+1}$ L^2 projection of $\left\{\mathbb{1}_{S_m^i}\right\}_m$ onto $\mathbb{P}^k$

Linear advection of a composite signal

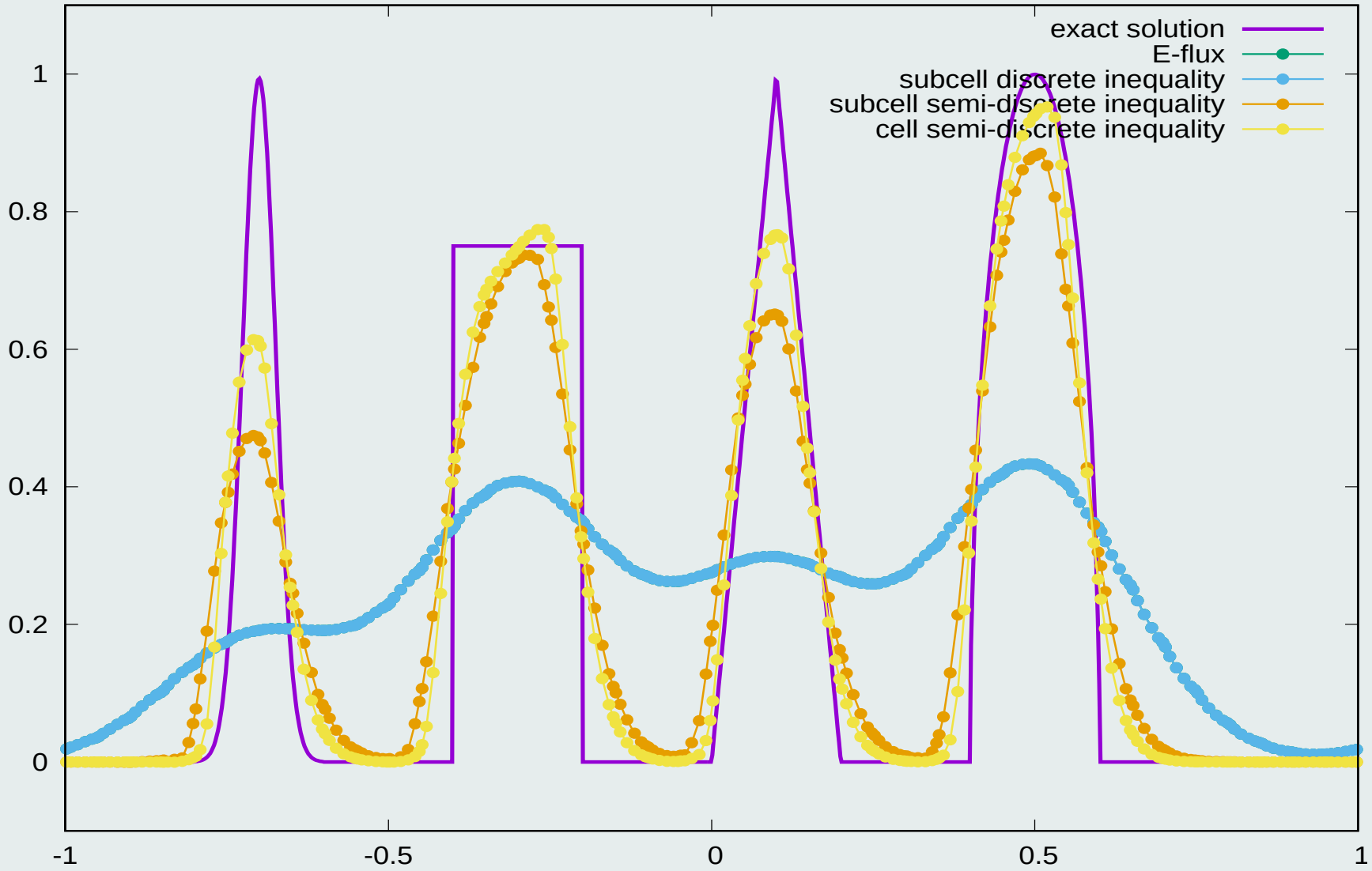

Figure : $\mathbb{P}^5$-DG/FV solutions on 40 cells: submean values

Non-linear Euler compressible gas dynamics equations

- $\partial_t \boldsymbol{V} + \nabla_x \cdot \boldsymbol{F}(\boldsymbol{V}) = \boldsymbol{0}$
- $\boldsymbol{V} = \begin{pmatrix} \rho \\ \boldsymbol{q} \\ E \end{pmatrix}$ conservative variables
- $\boldsymbol{F}(\boldsymbol{V}) = \begin{pmatrix} \boldsymbol{q} \\ \dfrac{\boldsymbol{q} \otimes \boldsymbol{q}}{\rho} + p\, I_d \\ (E+p)\dfrac{\boldsymbol{q}}{\rho} \end{pmatrix}$ flux function
- $p := p(\boldsymbol{V}) = (\gamma - 1)\left(E - \frac{1}{2}\frac{\|\boldsymbol{q}\|^2}{\rho}\right)$ equation of state

Monolithic subcell DG/FV scheme property

- Positivity of the density and internal energy, at the subcell scale

Definitions

- $\widehat{\boldsymbol{F}}_{m+\frac{1}{2}} := \boldsymbol{F}_{m+\frac{1}{2}} + \Theta_{m+\frac{1}{2}} \underbrace{\left(\widehat{\boldsymbol{F}}_{m+\frac{1}{2}} - \boldsymbol{F}_{m+\frac{1}{2}}\right)}_{\Delta \boldsymbol{F}_{m+\frac{1}{2}}}$ convex blended flux
- $\Theta_{m+\frac{1}{2}} = \begin{pmatrix} \theta^{\rho}_{m+\frac{1}{2}} & 0 & 0 \\ 0 & \theta^{q}_{m+\frac{1}{2}} & 0 \\ 0 & 0 & \theta^{E}_{m+\frac{1}{2}} \end{pmatrix}$
- $\boldsymbol{F}_{m+\frac{1}{2}} = \dfrac{\boldsymbol{F}(\overline{\boldsymbol{V}}_m) + \boldsymbol{F}(\overline{\boldsymbol{V}}_{m+1})}{2} - \dfrac{\gamma_{m+\frac{1}{2}}}{2} \left(\overline{\boldsymbol{V}}_{m+1} - \overline{\boldsymbol{V}}_m\right)$

Positivity of the density

- $\theta^{\rho}_{m+\frac{1}{2}} = \theta^{\rho\,(1)}_{m+\frac{1}{2}}\, \theta_{m+\frac{1}{2}}$

$$\theta^{\rho\,(1)}_{m+\frac{1}{2}} \leq \min\left(1, \left|\frac{\gamma_{m+\frac{1}{2}}}{\Delta F^{\rho}_{m+\frac{1}{2}}}\right| \rho^{*}_{m+\frac{1}{2}}\right)$$

Positivity of the internal energy

- $A_{m+\frac{1}{2}} = \dfrac{1}{(\gamma_{m+\frac{1}{2}})^2}\left(\dfrac{1}{2}\left(\Delta F^q_{m+\frac{1}{2}}\right)^2 - \theta^{\rho\,(1)}_{m+\frac{1}{2}}\Delta F^\rho_{m+\frac{1}{2}}\,\Delta F^E_{m+\frac{1}{2}}\right)$
- $B_{m+\frac{1}{2}} = \dfrac{1}{\gamma_{m+\frac{1}{2}}}\left(q^*_{m+\frac{1}{2}}\,\Delta F^q_{m+\frac{1}{2}} - \rho^*_{m+\frac{1}{2}}\,\Delta F^E_{m+\frac{1}{2}} - \theta^{\rho\,(1)}_{m+\frac{1}{2}}\,E^*_{m+\frac{1}{2}}\,\Delta F^\rho_{m+\frac{1}{2}}\right)$
- $M_{m+\frac{1}{2}} = \rho^*_{m+\frac{1}{2}}\,E^*_{m+\frac{1}{2}} - \frac{1}{2}\left(q^*_{m+\frac{1}{2}}\right)^2$

$$\theta_{m+\frac{1}{2}} \leq \min\left(1,\ \frac{M_{m+\frac{1}{2}}}{\left|B_{m+\frac{1}{2}}\right| + \max\left(0, A_{m+\frac{1}{2}}\right)}\right)$$

- $\theta^\rho_{m+\frac{1}{2}} = \theta^{\rho\,(1)}_{m+\frac{1}{2}}\,\theta_{m+\frac{1}{2}}, \quad \theta^q_{m+\frac{1}{2}} = \theta_{m+\frac{1}{2}}, \quad \theta^E_{m+\frac{1}{2}} = \theta_{m+\frac{1}{2}}$

A. Rueda-Ramírez, B. Bolm, D. Kuzmin and **G. Gassner**, *Monolithic Convex Limiting for Legendre-Gauss-Lobatto Discontinuous Galerkin Spectral Element Methods*. Arxiv, 2023.

LMP

$$\overline{v}_m^{n+1} \in \mathrm{I}\left(\overline{v}_{m-1}^n,\ v_{m-\frac{1}{2}}^*,\ \overline{v}_m^n,\ v_{m+\frac{1}{2}}^*,\ \overline{v}_{m+1}^n\right)$$

- $v \in \{\rho,\ q,\ E\}$ conservative variable

- $\widetilde{v_{m+\frac{1}{2}}}^{-} \in [\alpha_m,\ \beta_m] := \mathrm{I}\left(\overline{v}_{m-1}^n,\ v_{m-\frac{1}{2}}^*,\ \overline{v}_m^n,\ v_{m+\frac{1}{2}}^*,\ \overline{v}_{m+1}^n\right)$
- $\widetilde{v_{m+\frac{1}{2}}}^{+} \in [\alpha_{m+1},\ \beta_{m+1}] := \mathrm{I}\left(\overline{v}_m^n,\ v_{m+\frac{1}{2}}^*,\ \overline{v}_{m+1}^n,\ v_{m+\frac{3}{2}}^*,\ \overline{v}_{m+2}^n\right)$

$$\theta_{m+\frac{1}{2}} \leq \min\left(1,\ \left|D_{m+\frac{1}{2}}\right| \begin{cases} \min\left(\beta_{m+1} - v_{m+\frac{1}{2}}^*,\ v_{m+\frac{1}{2}}^* - \alpha_m\right) & \text{if } \Delta F_{m+\frac{1}{2}} > 0 \\ \min\left(\beta_m - v_{m+\frac{1}{2}}^*,\ v_{m+\frac{1}{2}}^* - \alpha_{m+1}\right) & \text{if } \Delta F_{m+\frac{1}{2}} < 0 \end{cases}\right)$$

- Smooth extrema relaxation to preserve accuracy

Sod shock tube test case

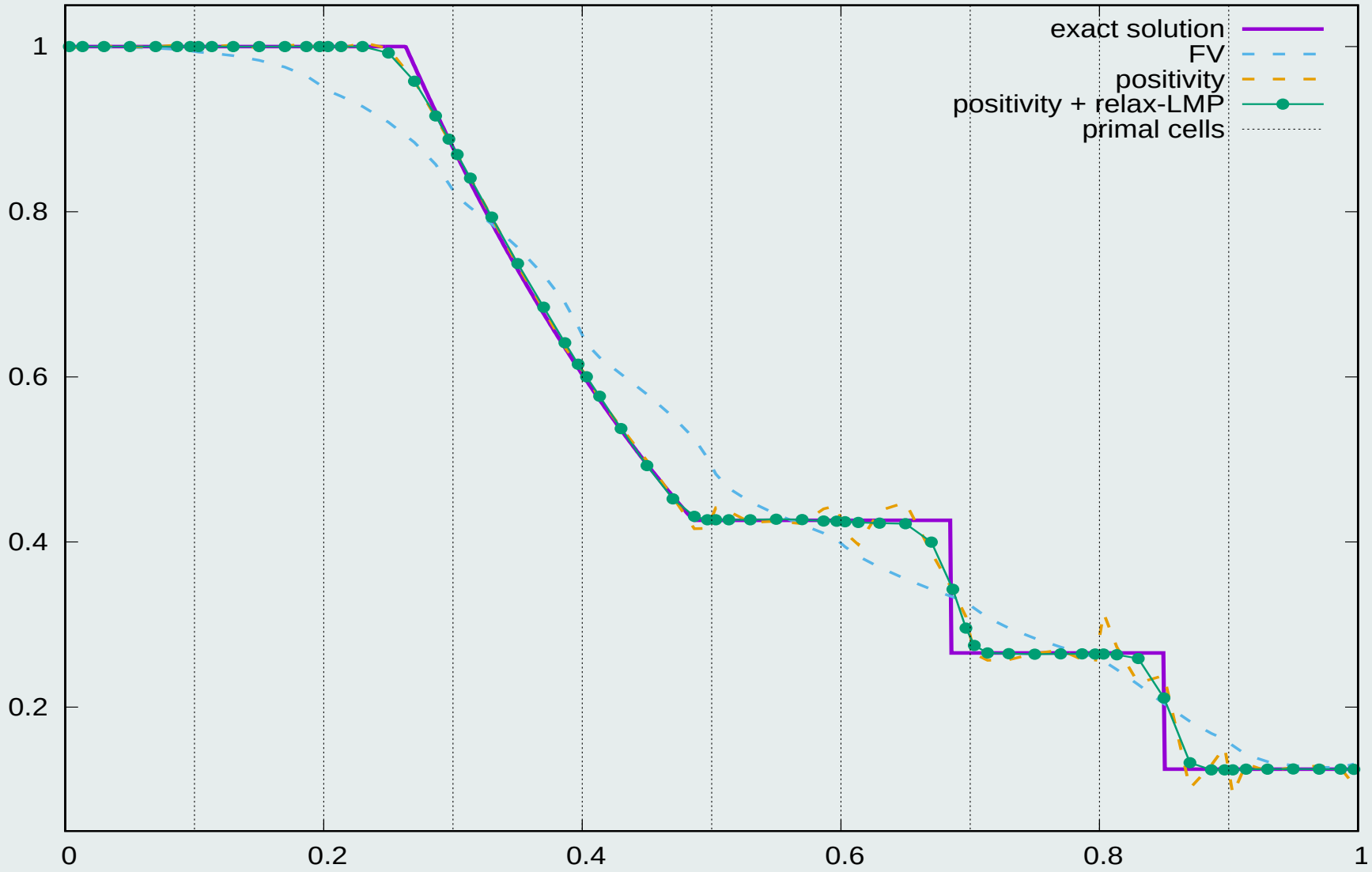

Figure : $\mathbb{P}^6$-DG/FV solutions on 10 cells: submean values

Sod shock tube test case

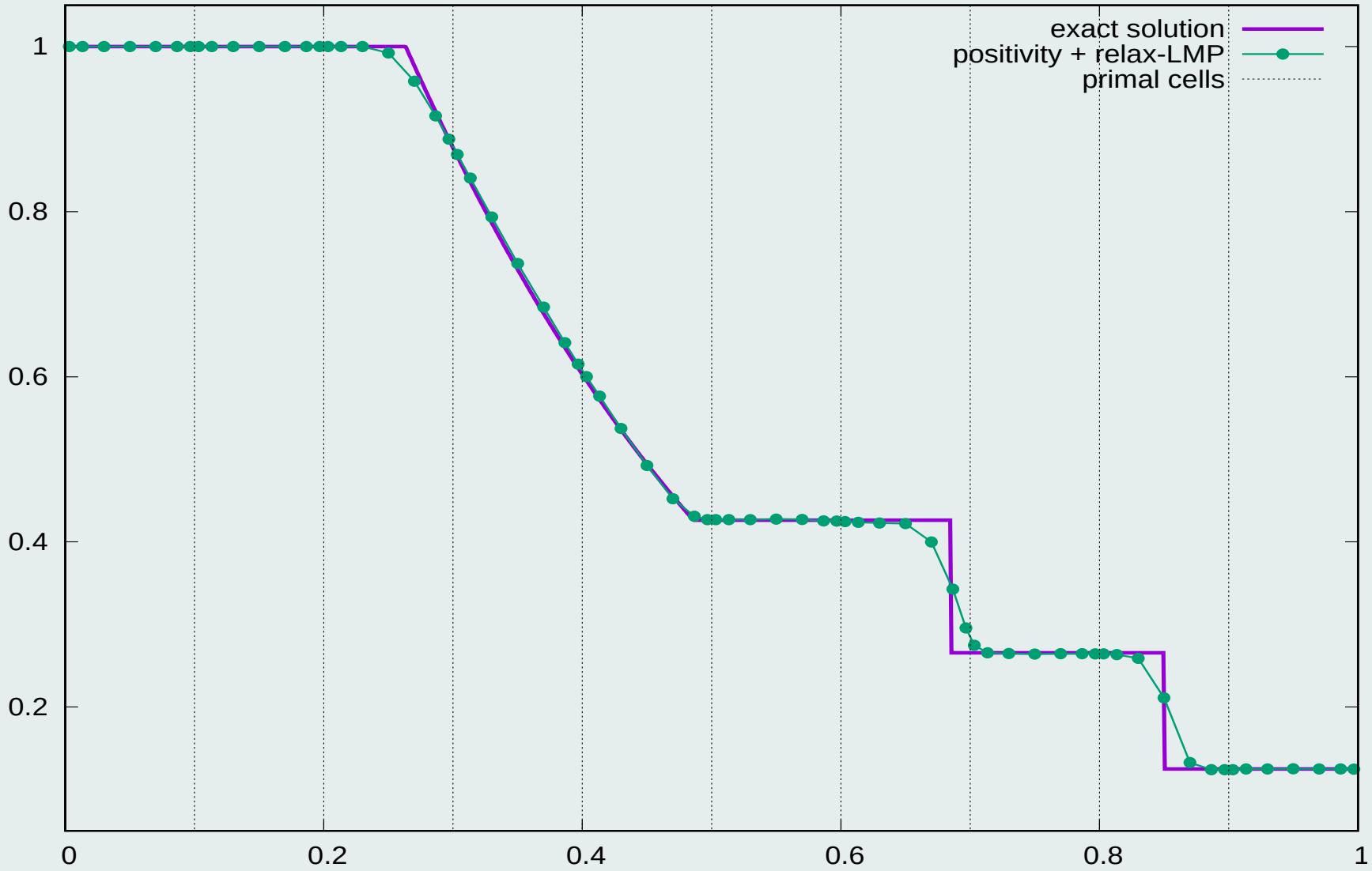

Figure : $\mathbb{P}^6$-DG/FV solutions on 10 cells: submean values

Smooth isentropic solution $\rho_0 = 1 + 0.9999999 \sin(2\pi x)$

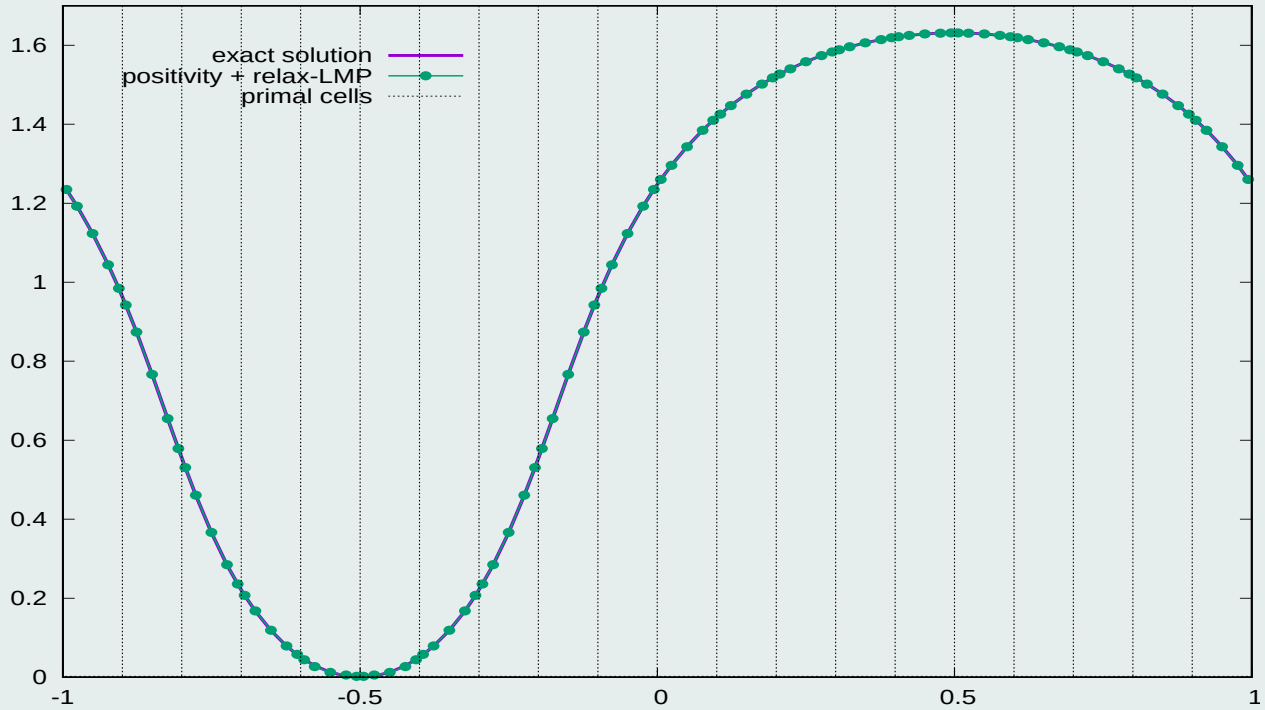

	L_1		L_2	
h	$E^h_{L_1}$	$q^h_{L_1}$	$E^h_{L_2}$	$q^h_{L_2}$
$\frac{1}{20}$	1.54E-5	4.01	2.04E-5	3.82
$\frac{1}{40}$	9.57E-7	4.89	1.45E-6	4.85
$\frac{1}{80}$	3.22E-8	4.84	5.00E-8	4.87
$\frac{1}{160}$	1.12E-9	-	1.71E-9	-

Table: Convergence rates computed on the pressure with a 5th-order DG/FV scheme

Different cell subdivisions $\mathbb{P}^3$

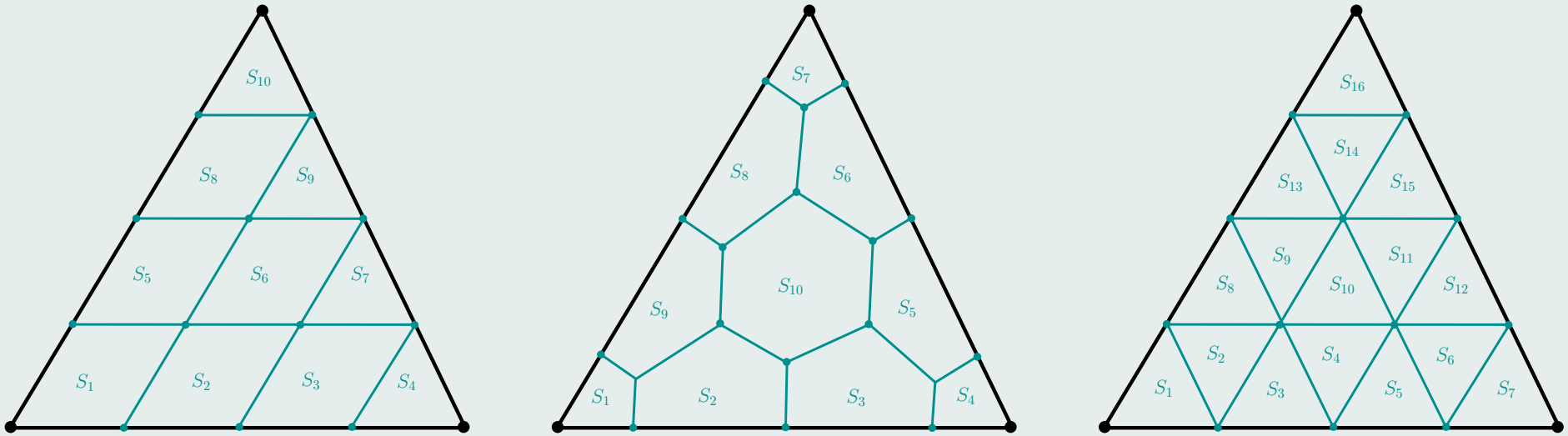

Figure : Examples of easily generalizable subdivisions for a triangle cell

Rotation of a composite signal after one full rotation

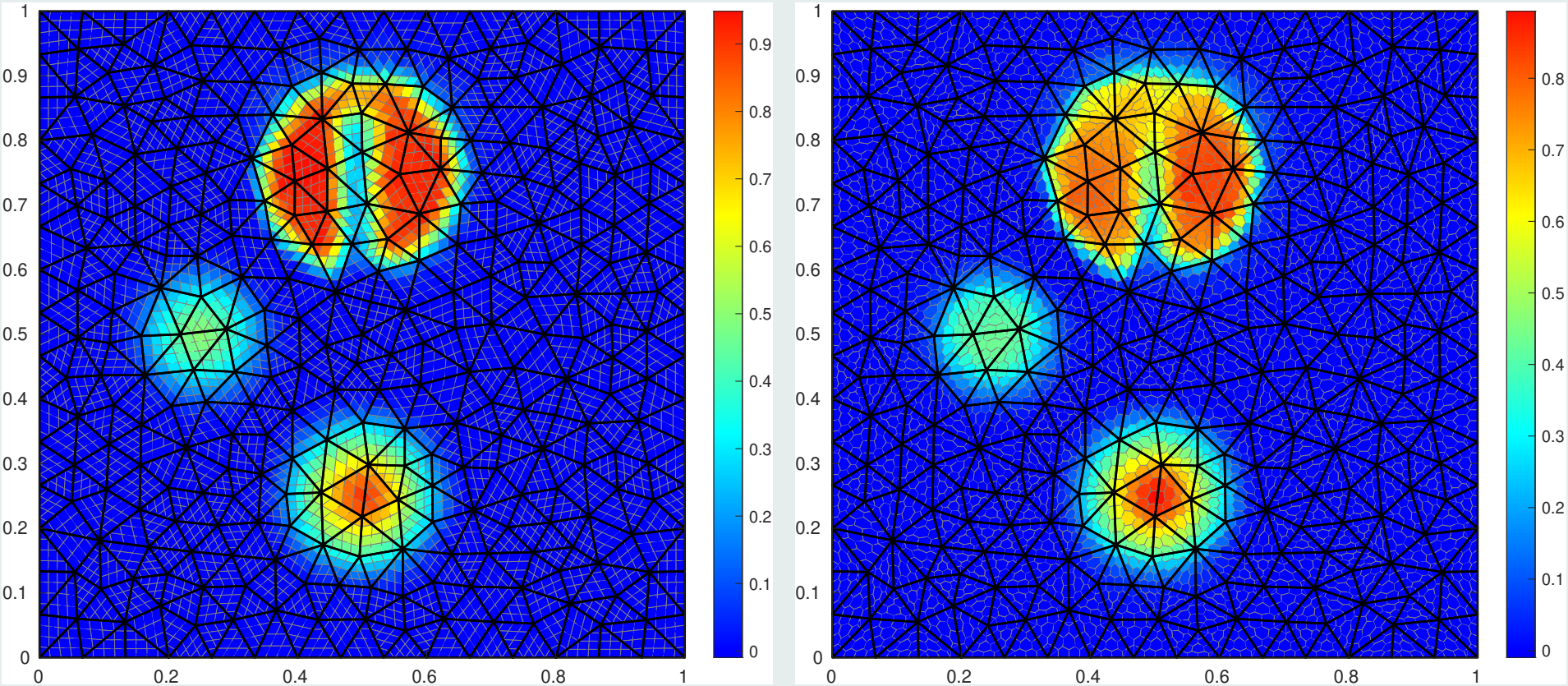

(a) Cartesian subdivision

(b) Polygonal subdivision

Figure : $\mathbb{P}^3$-DG/FV scheme with GMP and relaxed-LMP on 576 cells: subcells mean values

Rotation of a composite signal after one full rotation

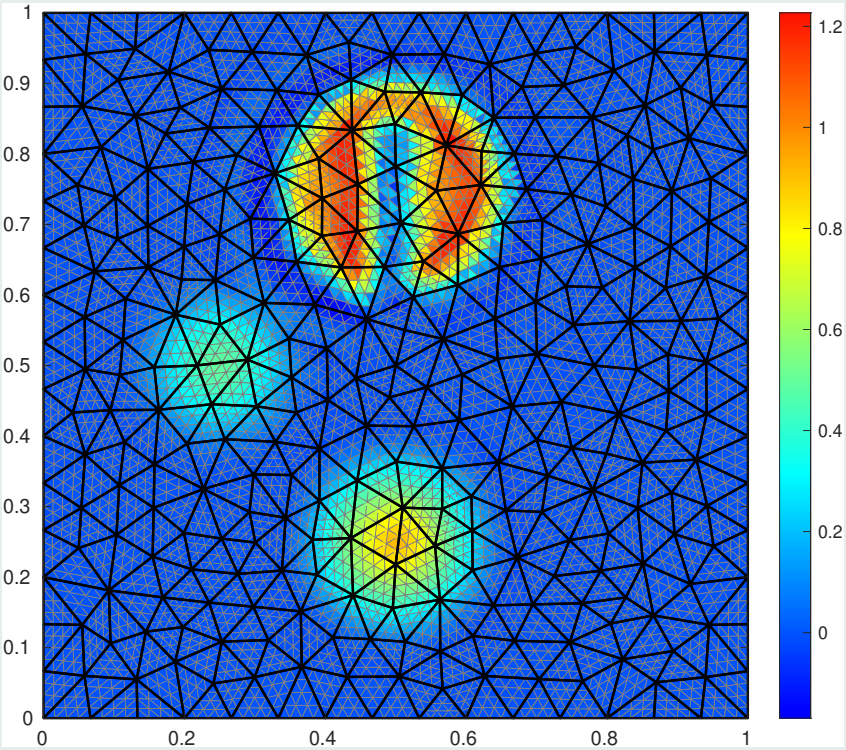

(a) Triangular subdivision

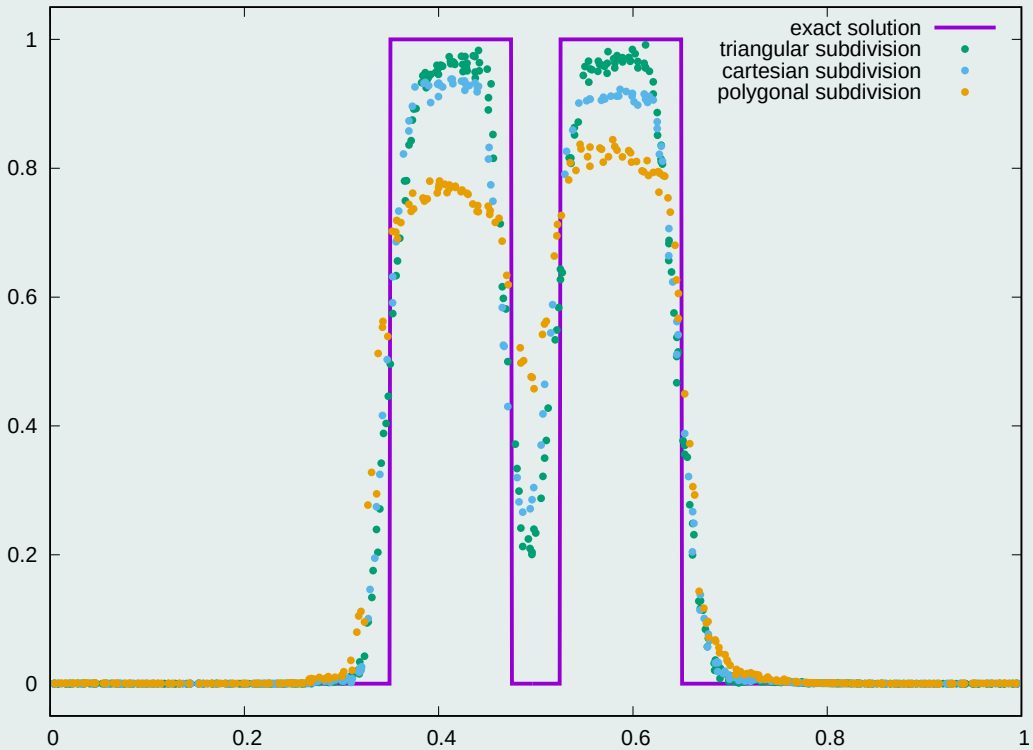

(b) solution profiles for $y = 0.75$

Figure : $\mathbb{P}^3$-DG/FV scheme with GLMP and relaxed-LMP on 576 cells

Cell subdivision impact

- **The subdivision does have an impact on the DG/FV scheme**
- **Much lesser for non-linear problems**

Burgers equation

$u_0(x, y) = \sin(2\pi\,(x + y))$

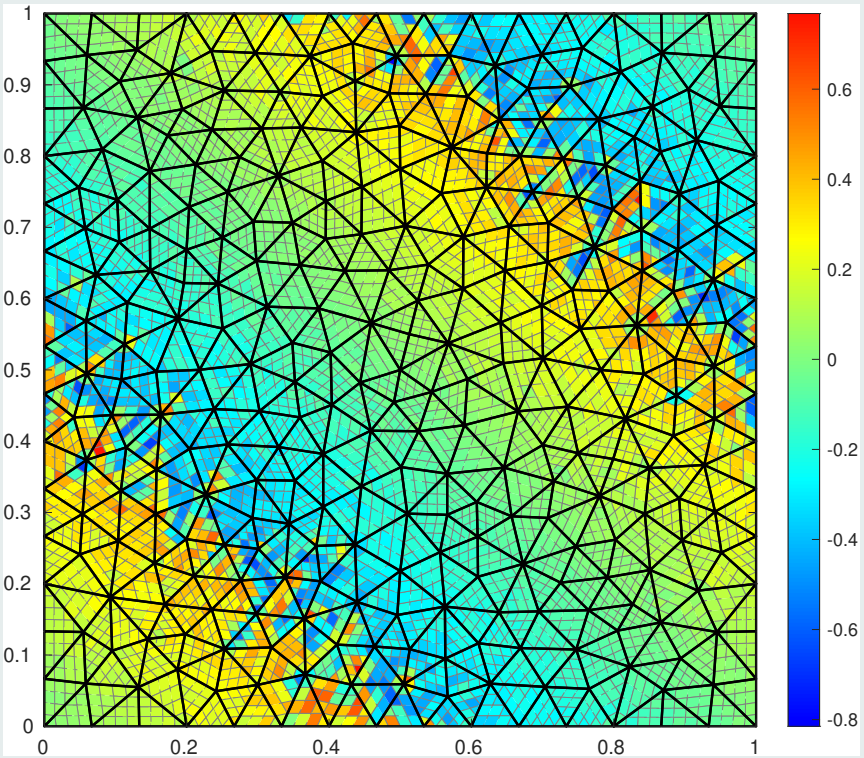

(a) DG

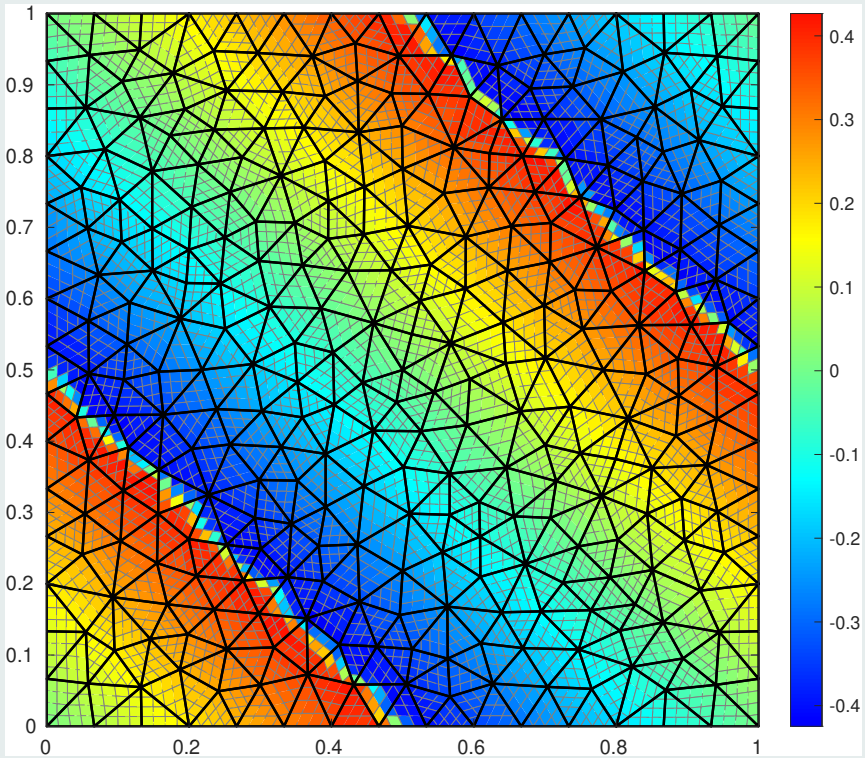

(b) GMP + relaxed-LMP

Figure : $\mathbb{P}^3$-DG/FV scheme on 576 cells: subcell mean values

Burgers equation

$u_0(x, y) = \sin(2\pi(x + y))$

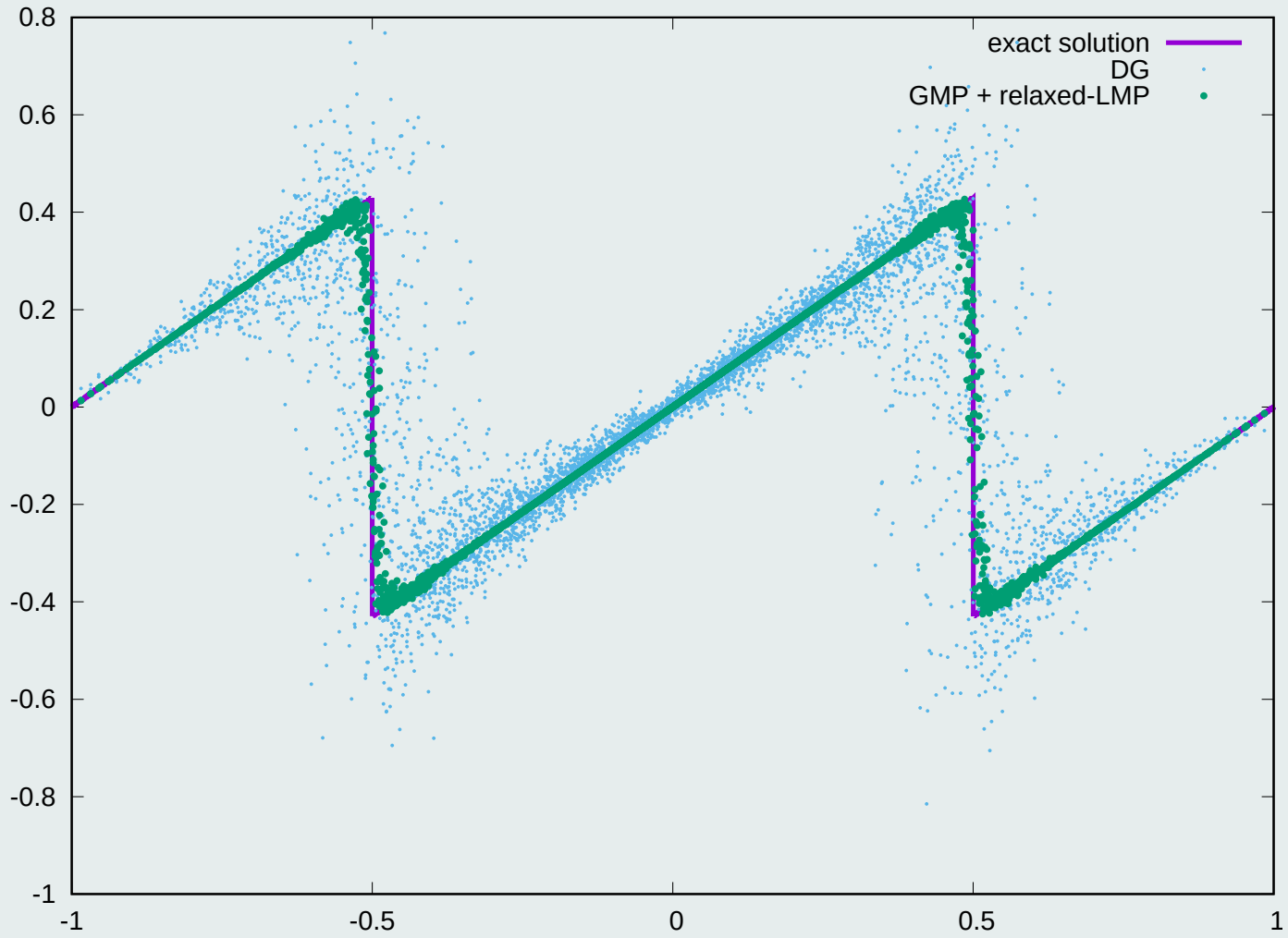

Figure : $\mathbb{P}^3$-DG/FV scheme with GMP and relaxed-LMP on a 576 cells mesh at $t = 0.5$: submean values versus $(x + y - 1)$ coordinate

Burgers equation

$u_0(x, y) = \sin(2\pi\,(x + y))$

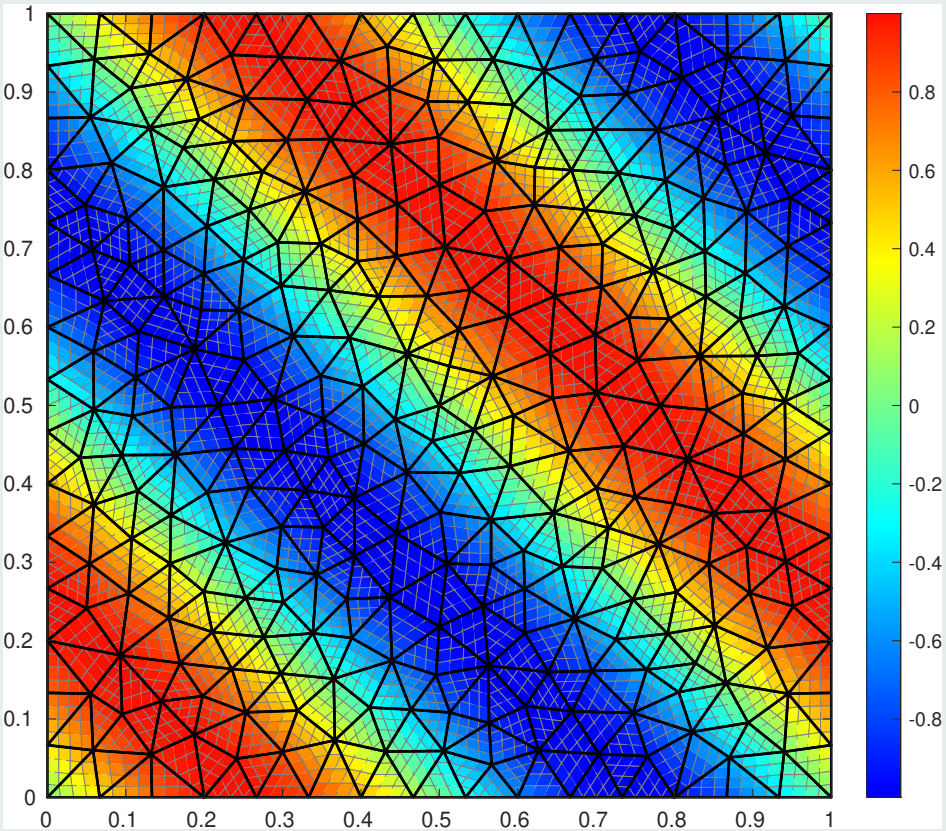

(a) Solution submean values

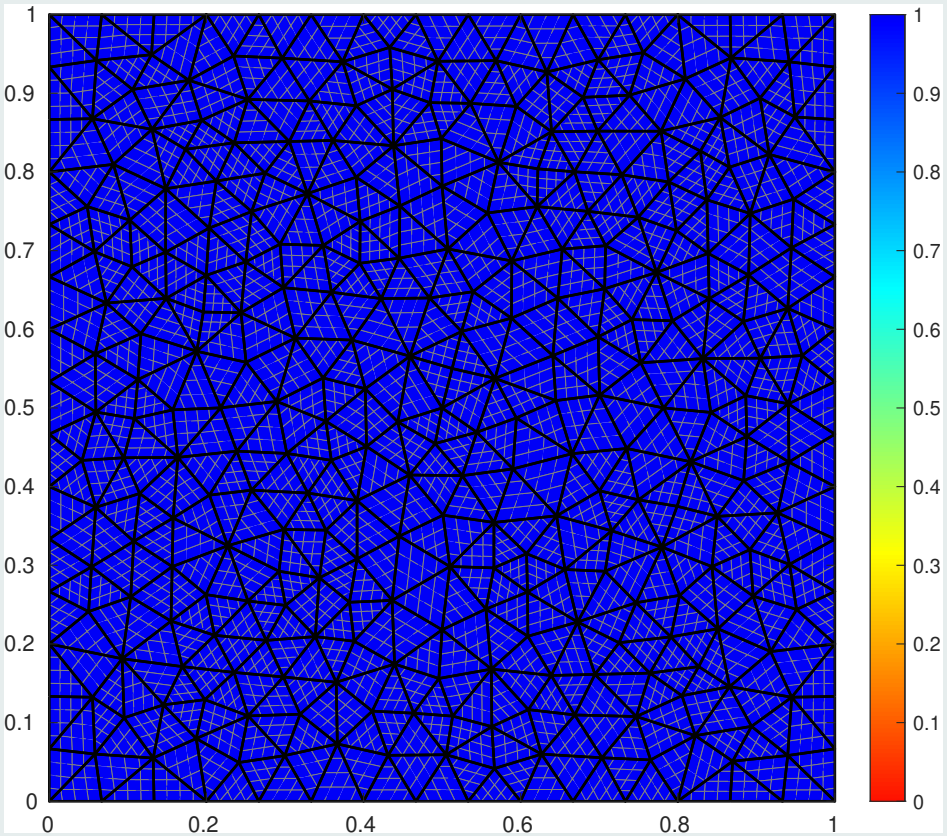

(b) Blending coefficients

Figure : $\mathbb{P}^3$-DG/FV scheme with GMP and relaxed-LMP on 576 cells

Sedov point blast problem in cylindrical geometry

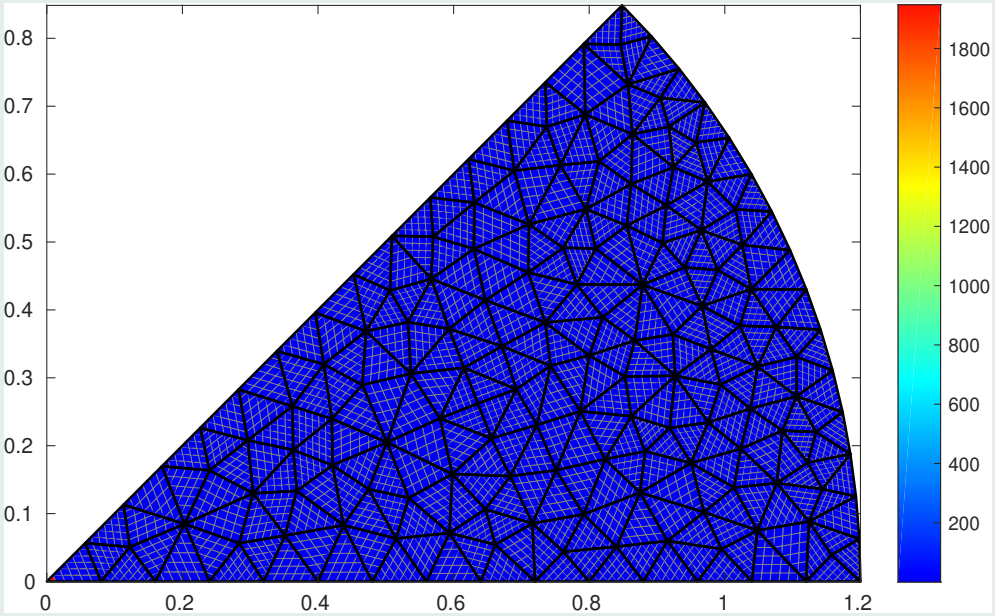

(a) Energy map

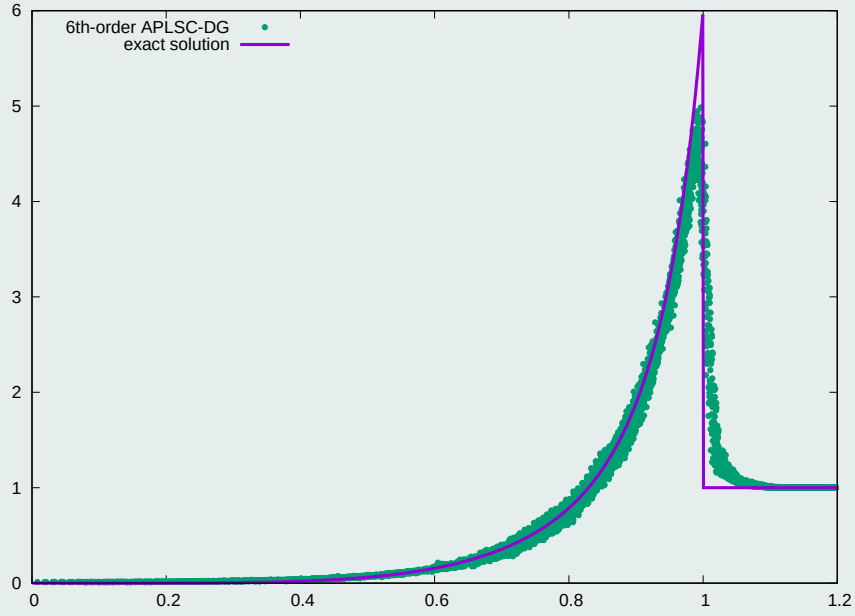

(b) Density profile

Figure : 6th-order APLSC-DG on a 271 cells mesh at $t = 1$

A Mach 3 wind tunnel with a step

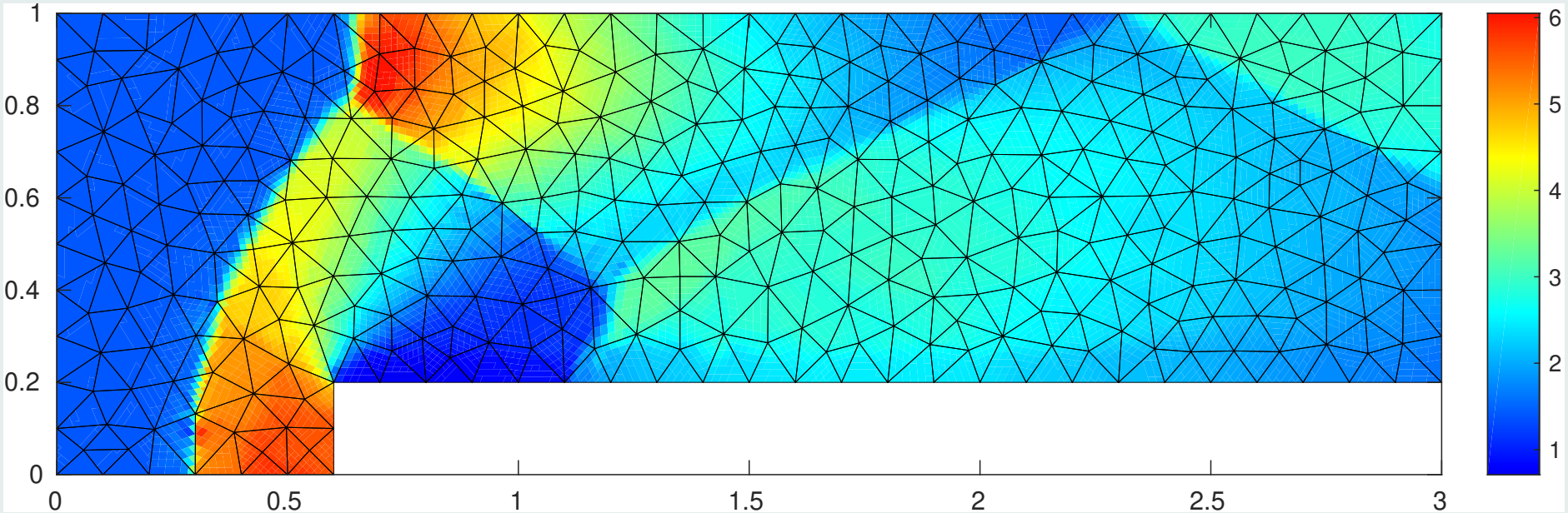

Figure : 6th-order APLSC-DG solution for the facing step problem on 680 cells at $t = 4$: submean density map

2D non-linear shallow water equations - prebalanced formulation

- $\partial_t \boldsymbol{V} + \nabla_x \cdot \boldsymbol{F}(\boldsymbol{V}, b) = \boldsymbol{B}(\boldsymbol{V}, \nabla_x b)$
- $\boldsymbol{V} = \begin{pmatrix} \eta \\ \boldsymbol{q} \end{pmatrix}$ conservative variables
- $\boldsymbol{B}(\boldsymbol{V}, \partial_x b) = \begin{pmatrix} 0 \\ -g\,\eta\,\nabla_x b \end{pmatrix}$ source term
- $\boldsymbol{F}(\boldsymbol{V}, b) = \begin{pmatrix} \boldsymbol{q} \\ \dfrac{\boldsymbol{q} \otimes \boldsymbol{q}}{\eta - b} + \dfrac{1}{2} g \left(\eta^2 - 2\,\eta\,b\right) I_d \end{pmatrix}$ flux function

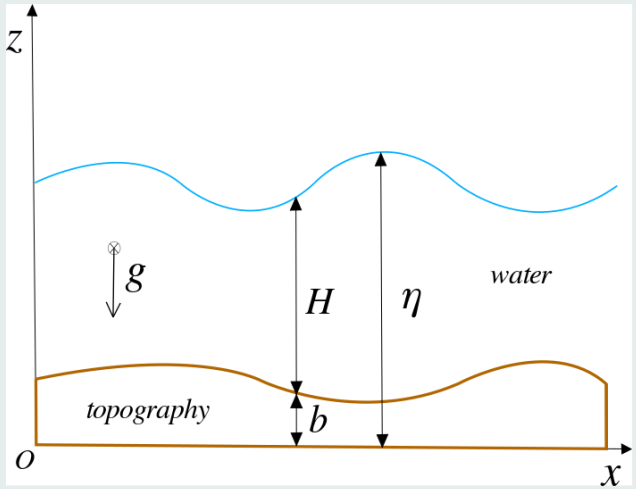

APLSC-DG scheme properties

- Positivity-preservation of the water height $H = \eta - b$, at the subcell scale
- Well-balancing property, at the subcell scale

Rock-wave interaction

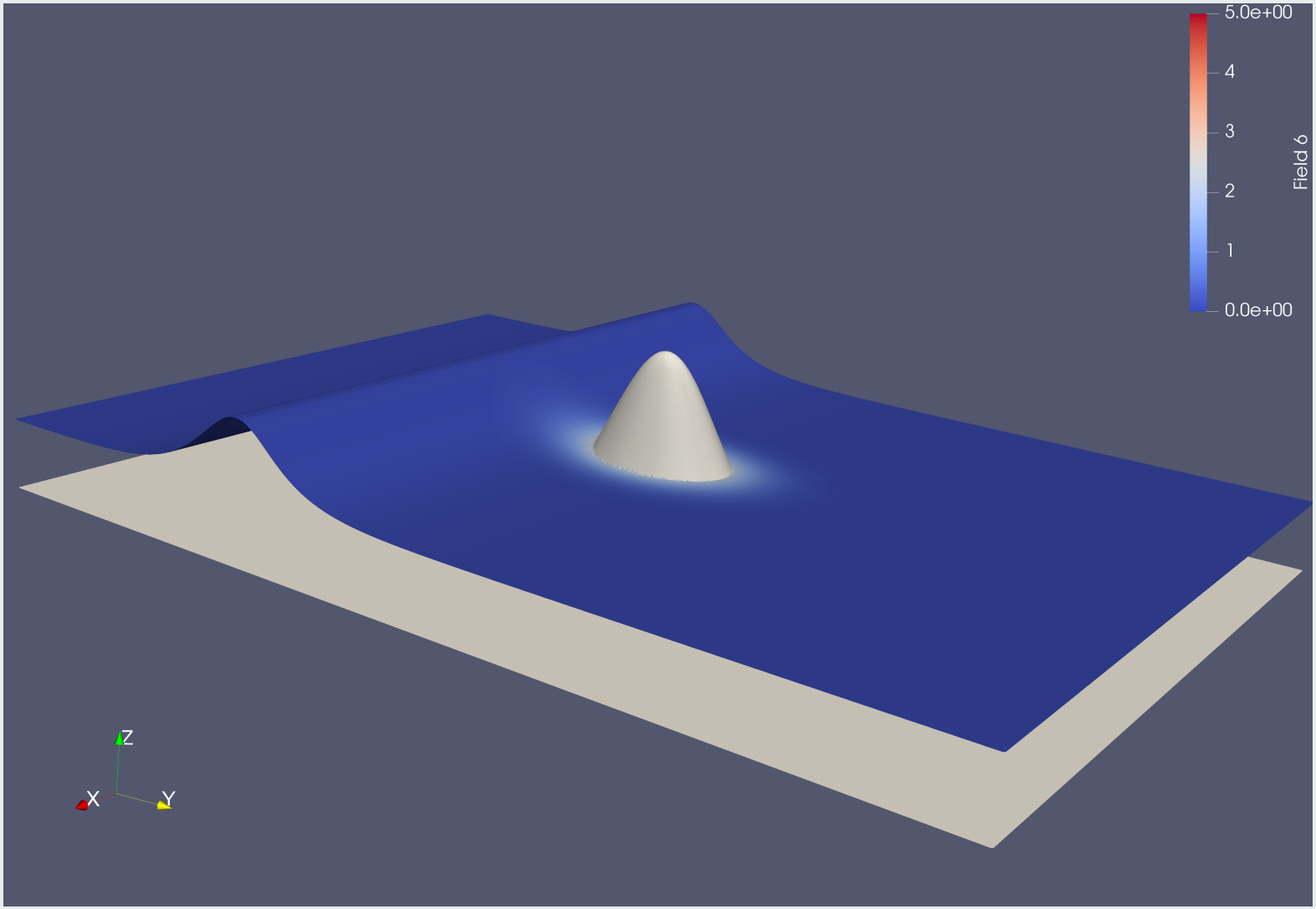

Figure : 3rd-order APLSC-DG on a 7000 cells mesh

Work in progress,

To be continued...

Articles on this topic

- **F. VILAR**, *A Posteriori Correction of High-Order DG Scheme through Subcell Finite Volume Formulation and Flux Reconstruction.* JCP, 387:245-279, 2018.
- **A. HAIDAR**, **F. MARCHE** AND **F. VILAR**, *A posteriori Finite-Volume local subcell correction of high-order discontinuous Galerkin schemes for the nonlinear shallow-water equations*. JCP, 452:110902, 2022.
- **F. VILAR** AND **R. ABGRALL**, *A posteriori local subcell correction of DG schemes through Finite Volume reformulation on unstructured grids.* SIAM JSC, article submitted, 2022.
- **A. HAIDAR**, **F. MARCHE** AND **F. VILAR**, *Free-boundary problems for wave-structure interactions in shallow-water: DG-ALE description and local subcell correction*. JSC, article submitted, 2023.
- **A. HAIDAR**, **F. MARCHE** AND **F. VILAR**, *A robust DG-ALE formulation for nonlinear shallow-water interactions with a floating object*. JSC, article submitted, 2023.

Articles on this topic

- **F. VILAR**, *A Posteriori Correction of High-Order DG Scheme through Subcell Finite Volume Formulation and Flux Reconstruction.* JCP, 387:245-279, 2018.
- **A. HAIDAR**, **F. MARCHE** AND **F. VILAR**, *A posteriori Finite-Volume local subcell correction of high-order discontinuous Galerkin schemes for the nonlinear shallow-water equations*. JCP, 452:110902, 2022.
- **F. VILAR** AND **R. ABGRALL**, *A posteriori local subcell correction of DG schemes through Finite Volume reformulation on unstructured grids.* SIAM JSC, article submitted, 2022.
- **A. HAIDAR**, **F. MARCHE** AND **F. VILAR**, *Free-boundary problems for wave-structure interactions in shallow-water: DG-ALE description and local subcell correction*. JSC, article submitted, 2023.
- **A. HAIDAR**, **F. MARCHE** AND **F. VILAR**, *A robust DG-ALE formulation for nonlinear shallow-water interactions with a floating object*. JSC, article submitted, 2023.

Cell subdivision: condition number of the projection matrix P_c

	$\mathbb{P}^0$	$\mathbb{P}^1$	$\mathbb{P}^2$	$\mathbb{P}^3$
Unif. struct. subdiv.	1	4	10.91	31.75
Non-unif. struct. subdiv.	1	4	9.52	29.28
Unif. polyg. subdiv.	1	2.87	8.73	27.89
Non-unif. polyg. subdiv.	1	2.87	8.19	26.94

Table: Projection matrix condition number for different orders and subdivisions